CAMS Service Evolution

CAMAERA

D9.1 Intercomparison and evaluation from different angles of the regional and global model, building on the 2022 CAMS2_40 regional model intercomparison – focus on AOD

Due date of deliverable	28/01/2026
Submission date	28/01/2026
File Name	CAMAERA-D9.1_AOD_v1.0.docx
Work Package /Task	WP9
Organisation Responsible of Deliverable	IOS-PIB/HYGEOS
Author name(s)	Jacek Kaminski / Joanna Struzewska / Tomasz Przybyła / Damian Mochocki / Samuel Remy / Rose-Cloé Meyer
Revision number	1.0
Status	
Dissemination Level	PU

The CAMAERA project (grant agreement No 101134927) is funded by the European Union.

1. Executive Summary

This report extends the previous evaluation of global and regional atmospheric composition models for PM10 and PM2.5 by assessing aerosol optical depth (AOD) for the year 2018. The analysis includes one global model, IFS-COMPO, and two regional models, GEM-AQ and MINNI. The regional simulations were driven by IFS-COMPO meteorological fields and chemical boundary conditions, while AOD was computed using model-specific optical schemes.

The study comprised a model intercomparison and an evaluation against observations. Spatial patterns of monthly mean AOD were compared between IFS-COMPO and GEM-AQ at high spatial resolution using a common emission dataset, while additional simulations with global emissions and the MINNI model were included to extend the comparison. Daily AOD at 550 nm was used to quantify similarities between models through pairwise Pearson correlation coefficients.

Modelled AOD fields were evaluated against ground-based observations from the AERONET network and satellite-based MODIS retrievals. The evaluation was restricted to periods and regions where observational data were available, applying appropriate filtering based on data availability and quality criteria.

This work provides a consistent framework for assessing AOD representation in global and regional atmospheric composition models and complements earlier analyses focused on particulate matter concentrations.

Table of Contents

1. Introduction

The objective of this annex report is to complement the analysis previously presented for PM10 and PM2.5 by including aerosol optical depth (AOD) derived from the outputs of one global (IFS-COMPO) and two regional atmospheric composition models (GEM-AQ and MINNI), with a particular focus on the year 2018.

Both regional models were driven by meteorological inputs from the Integrated Forecasting System global composition model (IFS-COMPO), provided at a temporal resolution of three hours. Chemical boundary conditions were also supplied by the IFS-COMPO global system at the same temporal resolution, ensuring dynamically consistent lateral forcing across the regional simulations.

Details of the optical modules implemented in the models are provided below, together with a brief description of the observational datasets used for the evaluation.

1.1 Optical schemes in the models

The optical modules described below differ in complexity, which may influence the resulting aerosol optical depth estimates.

In the IFS model AOD is computed online in the AER BDGTMSS routine. The mass extinction for each species (computed offline and stored as look-up tables in arrays) is multiplied by air density as well as the mass mixing ratio to obtain model-level extinction for each aerosol species, which is then summed over all aerosol species to obtain total aerosol extinction at each model level. Vertical integration is then carried out at each of the 20 following wavelengths: 340, 355, 380, 400, 440, 469, 500, 532, 555, 645, 670, 800, 858, 865, 1020, 1064, 1240, 1640, 2130 and 10000 nm. The aerosol absorption is computed for each species and each model level by multiplying the simulated aerosol extinction by (1 - SSA) where SSA is the single scattering albedo computed offline by the Mie code. Similarly to AOD, this is then summed over species.

In the GEM-AQ model the optical module allows the calculation of optical properties for five aerosol types: mineral dust, sulphate aerosols, organic aerosols, black carbon, and sea salt. The scheme uses backscattering coefficients derived for the NARCM model, which shares the same aerosol parameterizations as GEM-AQ, including dependencies on humidity, particle size, and wavelength. Aerosols are treated as an external mixture of homogeneous particle types, and the total optical depth is calculated as the sum of the contributions from individual aerosol species. The calculation proceeds by determining particle size and volume for each aerosol type (5 types) and size bins 12 bins), applying wavelength-dependent backscattering coefficients (defined for 14 discrete wavelengths - 340, 380, 440, 470, 500, 550, 670, 860, 870, 940, 1020, 1240, 1640, 2130 nm), and incorporating meteorological parameters to compute pressure changes across model layers. The resulting aerosol optical depth is calculated separately for each aerosol type and wavelength.

In the MINNI model the AOD@550 was calculated by integrating the aerosol extinction coefficient vertically from the surface to the top-of-atmosphere multiplying layer thickness at each vertical layer and 14 layers (top altitude 7040m), and extinction coefficients calculated for each layer (Colette et al., 2025). The extinction coefficient is the sum of extinction coefficients of Aitken and accumulation mode and standard value for Rayleigh extinction (0.01 km^{-1}). Aerosol extinction coefficient of each mode is

normalized by wavelength and total particle volume concentration of the mode using logarithm of their geometric standard deviation. These dimensionless extinction coefficients are computed using Mie parameters for modal mass median diameters according to the water mass fraction of aerosol and its corresponding real and imaginary parts of the refractive index, NR and NI. These indexes are estimated through a linear interpolation between "dry" state (1.5 - 0.01i) and pure water particle (1.33 - 0.0i).

1.2 AOD@550 - MODIS

The MODIS MAIAC Aerosol Optical Depth (AOD) product (MCD19A2) at 550 nm was obtained from the NASA Earthdata repository (https://www.earthdata.nasa.gov/) using the EarthAccess Python library and processed to generate monthly mean AOD values for 2018. Daily HDF files, each corresponding to a specific MODIS tile, were read and quality-filtered to remove unreliable observations. Pixels affected by clouds or with low retrieval quality were excluded based on the AOD quality assurance (QA) flags, which encode retrieval confidence (0–3, with lower values indicating higher quality) and cloud contamination indicators. Only pixels with high retrieval quality (QA ≤ 1) and low cloud contamination (cloud indicator ≤ 1) were retained. The native sinusoidal coordinates of each tile, with a nominal pixel size of approximately 1 km at the equator, were transformed to geographic coordinates (WGS84), and the approximate area of each MODIS pixel was calculated to allow area-weighted aggregation. Valid pixels were binned into a regular 0.1° × 0.1° latitude-longitude grid covering the study region, and monthly AOD values in each grid cell were computed as area-weighted averages.
Localized artifacts visible in parts of North Africa and the Middle East are consistent with known limitations of the MAIAC AOD product reported in previous studies and official product documentation (https://amt.copernicus.org/articles/11/5741/2018). These effects are most likely related to the performance of the aerosol retrieval algorithm over very bright desert surfaces or regional aerosol model boundaries, and may be further emphasized by reprojecting MODIS tiles from the native sinusoidal grid to a regular latitude–longitude grid.

1.3 AOD@550 - AERONET

The Aerosol Robotic Network (AERONET) was used as a source of ground based AOD observation in 2018 (https://aeronet.gsfc.nasa.gov/). AOD measurements provided by AERONET are processed using a centralized calibration and inversion framework, ensuring consistency across the network. In this report the Level 2.0 data representing cloud-screened and quality-assured observations are used for selected stations in Europe. Data were downloaded for hourly, daily and monthly means.

The analysis was based on hourly AERONET observations and corresponding hourly AOD outputs from the air quality models, which enabled direct temporal comparison between measurements and simulations. Daily mean values were calculated from all valid AERONET observations available for a given day. Model data were averaged only over the hours for which AERONET observations were available, ensuring temporal consistency between observations and simulations. Weekly and monthly averages were subsequently derived from the daily means.

Statistical evaluation was performed using standard performance metrics, including mean bias (MB), root mean square error (RMSE), Pearson correlation coefficient (R), and fractional bias

(FB). Statistics were calculated only for time steps where both model and observational data were available. All metrics were computed consistently for station-based and regional-mean time series.

2. Model intercomparison

The section 2.1 presents a comparison of spatial AOD patterns simulated by IFS-COMPO at high resolution using CAMS regional emissions and by the GEM-AQ model at a corresponding resolution with the same emission dataset. The MINNI model was not included in this comparison in order to simplify the analysis and due to the simplified formulation of AOD calculations.

In section 2.2, two other model runs were introduced: IFS-COMPO at high resolution with global emissions, and MINNI. To assess similarities in model performance, Pearson correlation coefficients were calculated between each pair of models—MINNI and GEM-AQ, GEM-AQ and IFS-COMPO, and IFS-COMPO and MINNI—using daily AOD at 550 nm over Europe.

2.1 Spatial pattern

Monthly mean AOD fields were calculated without applying any spatial masking; all grid-point values were used to compute the monthly averages. The maps, therefore, represent modelled AOD fields directly, without filtering for observational coverage.

The comparison between IFS-COMPO and GEM-AQ shows systematically lower AOD values in GEM-AQ, particularly during winter months. Over the Atlantic Ocean, AOD values are comparable in winter, while from April to September, the AOD over the Atlantic is substantially higher in IFS-COMPO. This may be related to long-range transport of aerosols associated with biomass burning from North America, which is not included in GEM-AQ for AOD calculations, as biomass burning emissions are introduced only as total PMWF.

A similar behavior of models is observed over North Africa, indicating comparable contributions of dust emissions. In some months, particularly April and May, AOD over the Sahara is higher in GEM-AQ, whereas in July and August the IFS-COMPO simulations show higher AOD values than GEM-AQ. The largest differences occur over Europe, where, for the GEM-AQ, the AOD is lower for most months. Comparable spatial patterns between the two models are reproduced mainly in March, April, and May.

	IFS	GEM-AQ
January	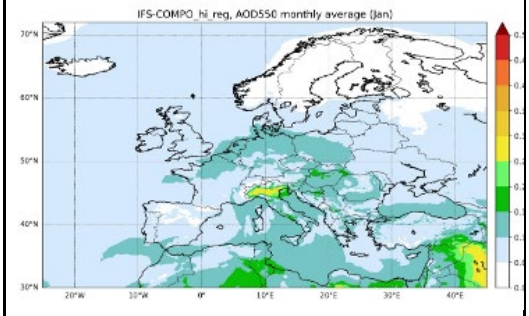	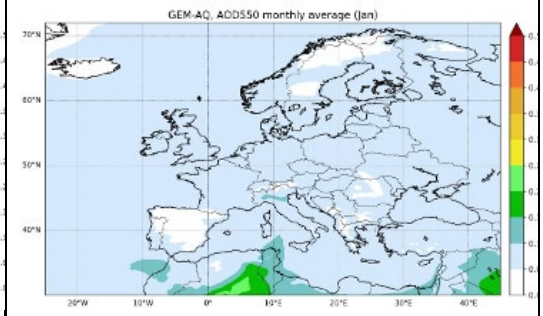
February	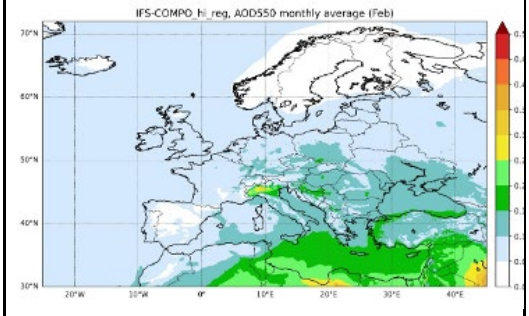	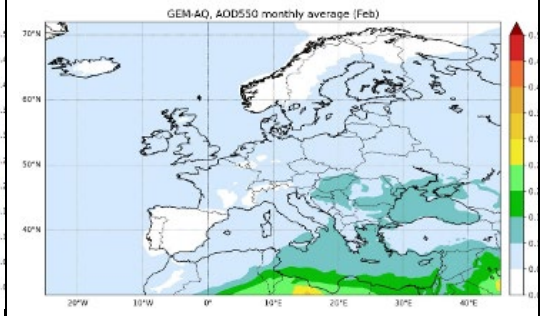
March	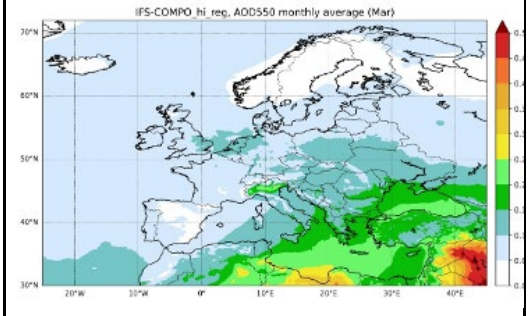	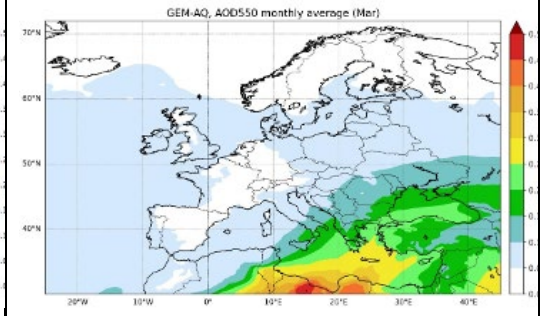
April	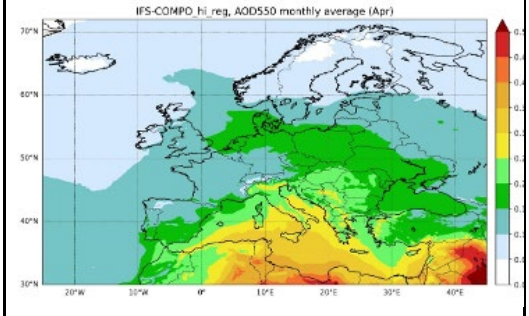	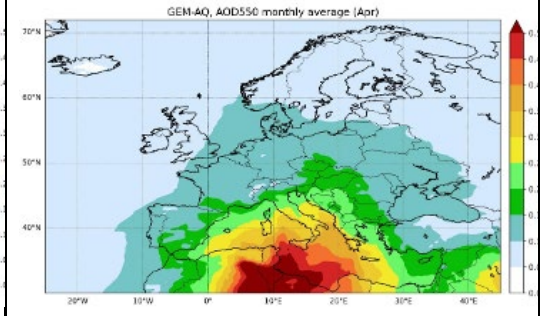
May	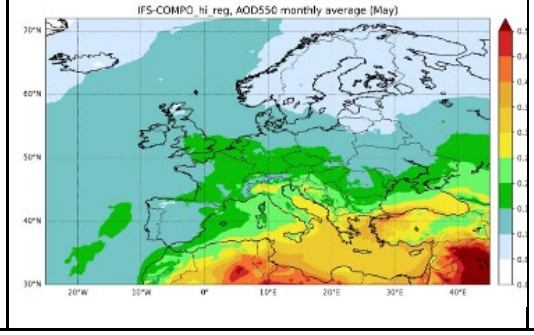	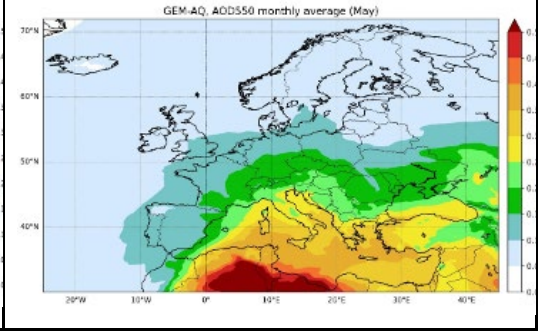

June	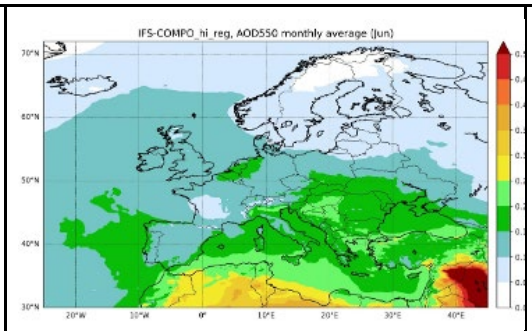	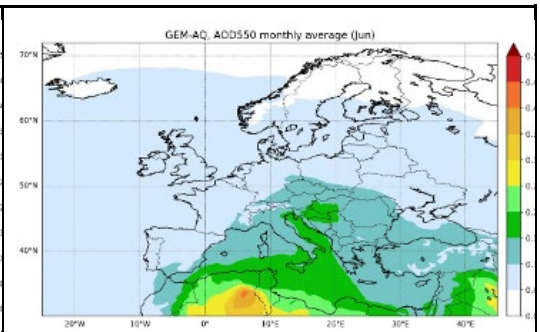
July	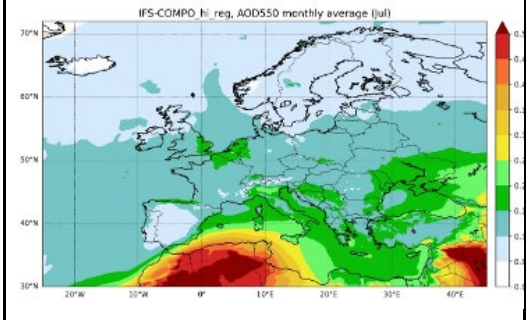	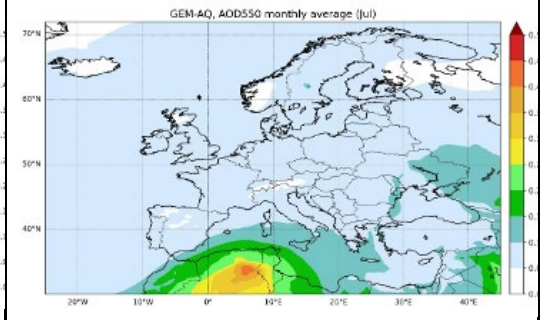
August	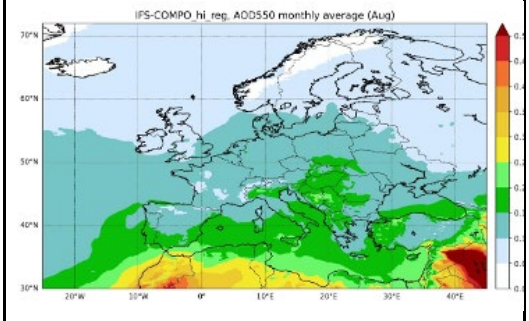	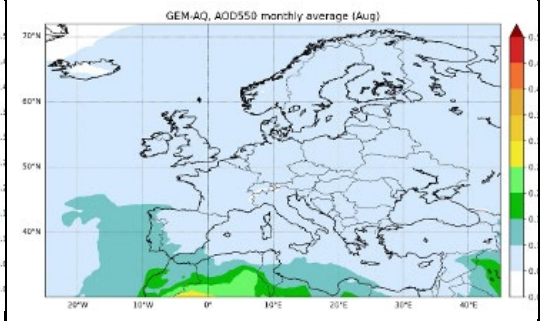
Septembe r	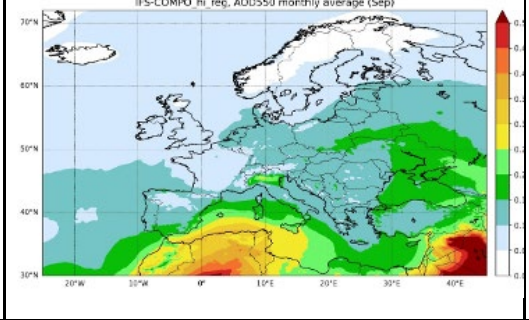	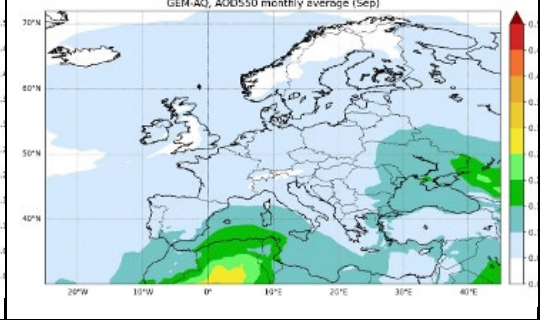
October	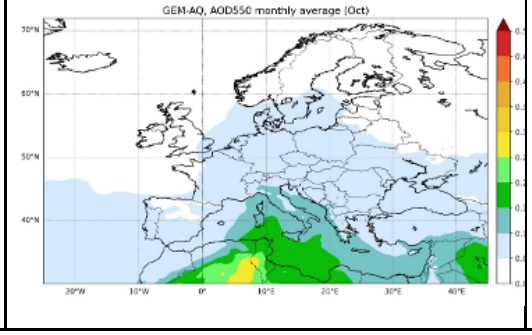	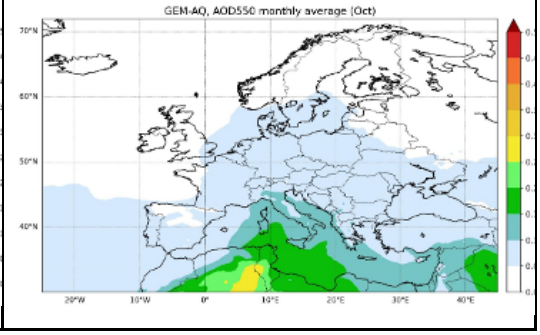

November	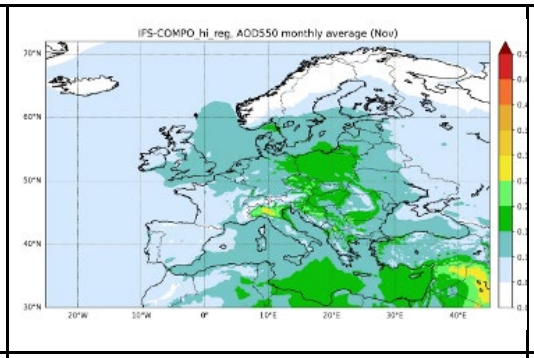	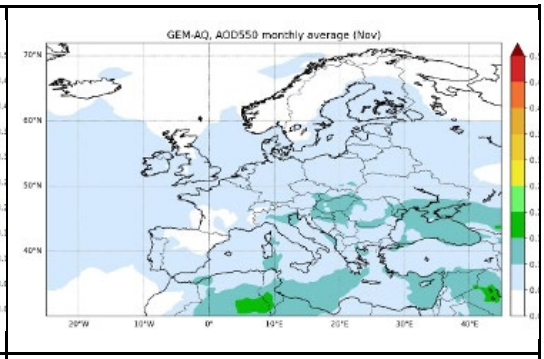
December	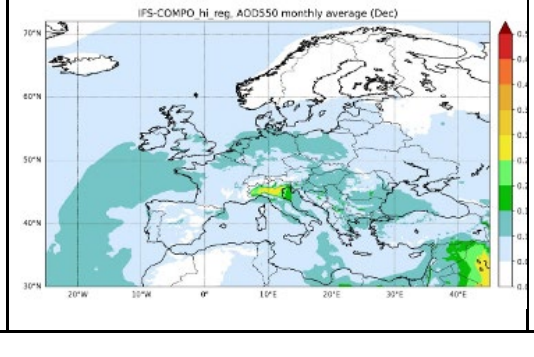	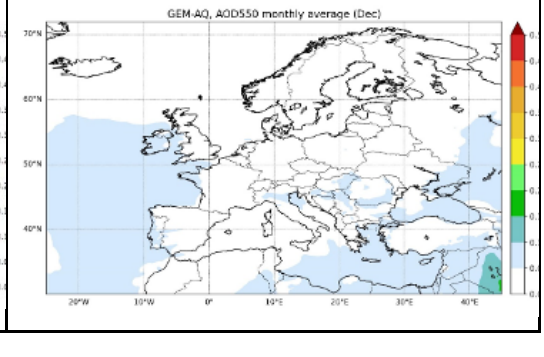

Figure 1. AOD@550 calculated with the IFS-COMPO results (left panel) and GEM-AQ results (right panel) as a monthly mean (no filter applied)

2.2 Spatial correlation

Analysis of the daily correlations shows that certain periods exhibit high agreement between models. Specifically:

- April to the end of July, as well as early February to early March: all model pairs show relatively high correlation across most model pairs,
- MINNI and IFS-COMPO: correlation remains high from September to the end of October.

Periods of large discrepancies in AOD calculations occur in January, mid-February, March, May, August, and November, indicating differences in model response during these months.

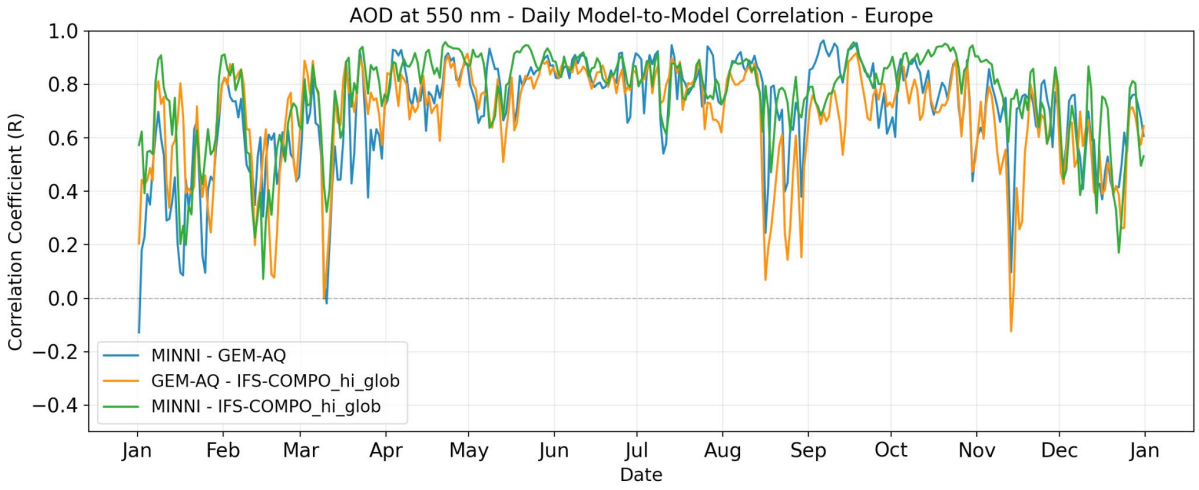

Figure 2. Daily spatial correlation coefficient between pairs of models

Considering annual and seasonal correlation coefficients:

- The correlation between MINNI and IFS-COMPO is stable throughout the year, with slightly lower values during the winter months.
- The correlation between GEM-AQ and IFS-COMPO varies between 0.60 and 0.74, with the highest correlation in spring (March–May) and the lowest in autumn (September–November)
- Overall, the correlation between MINNI and GEM-AQ is slightly higher than that between GEM-AQ and IFS-COMPO, which can be attributed to the use of the same emissions dataset in MINNI and GEM-AQ
- The lowest correlations involving IFS-COMPO occur in winter (December–February), while during the remaining months correlations are generally above 0.70.

These results suggest that there are common processes governing AOD, such as dust intrusions and anthropogenic emissions, which contribute to periods of high model agreement. The seasonal degradation in correlation indicates should be further investigated to understand the low correspondence between models.

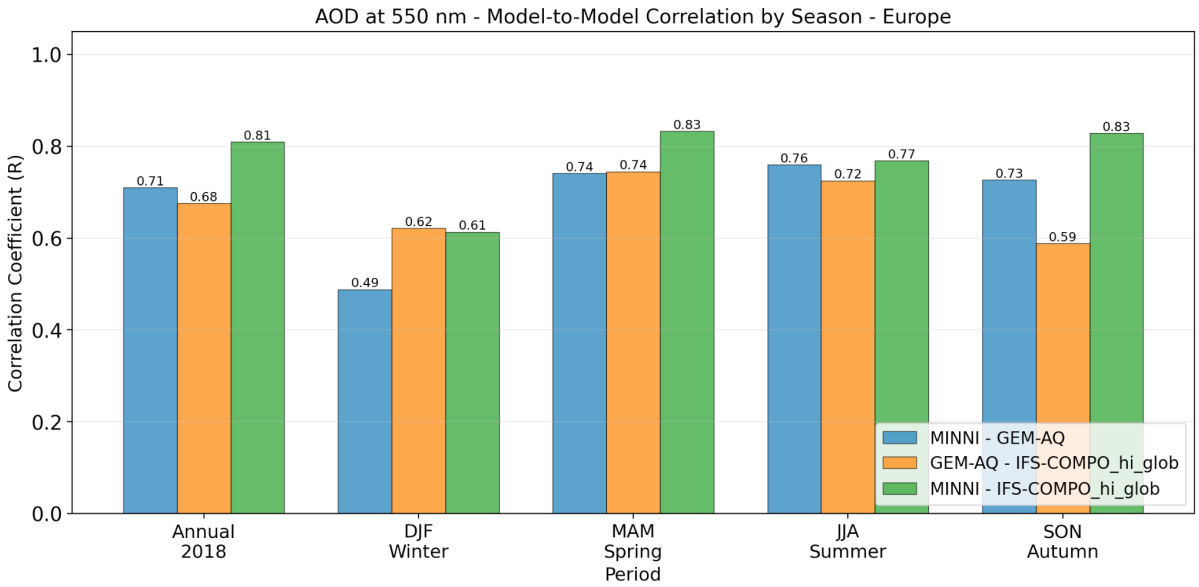

Figure 3. Annual and seasonal spatial correlation coefficient between pairs of models

3. AOD evaluation

For the evaluation, the high-resolution IFS-COMPO simulation with global emissions, as well as the GEM-AQ and MINNI results, were used. The comparison was performed against ground-based AERONET observations (Section 3.1) and MODIS satellite data (Section 3.2). Filtering was applied to include only periods and regions where observations were available.

To capture the diversity of atmospheric and geographical conditions across Europe, the model intercomparison study encompassed seven distinct regions. These regions were selected based on their contrasting climatological, topographical, and emission characteristics that are critical factors influencing the formation and dispersion of particulate matter. The inclusion of a broad geographic spread enhances the robustness of the evaluation and supports a better understanding of model performance under varying environmental contexts.

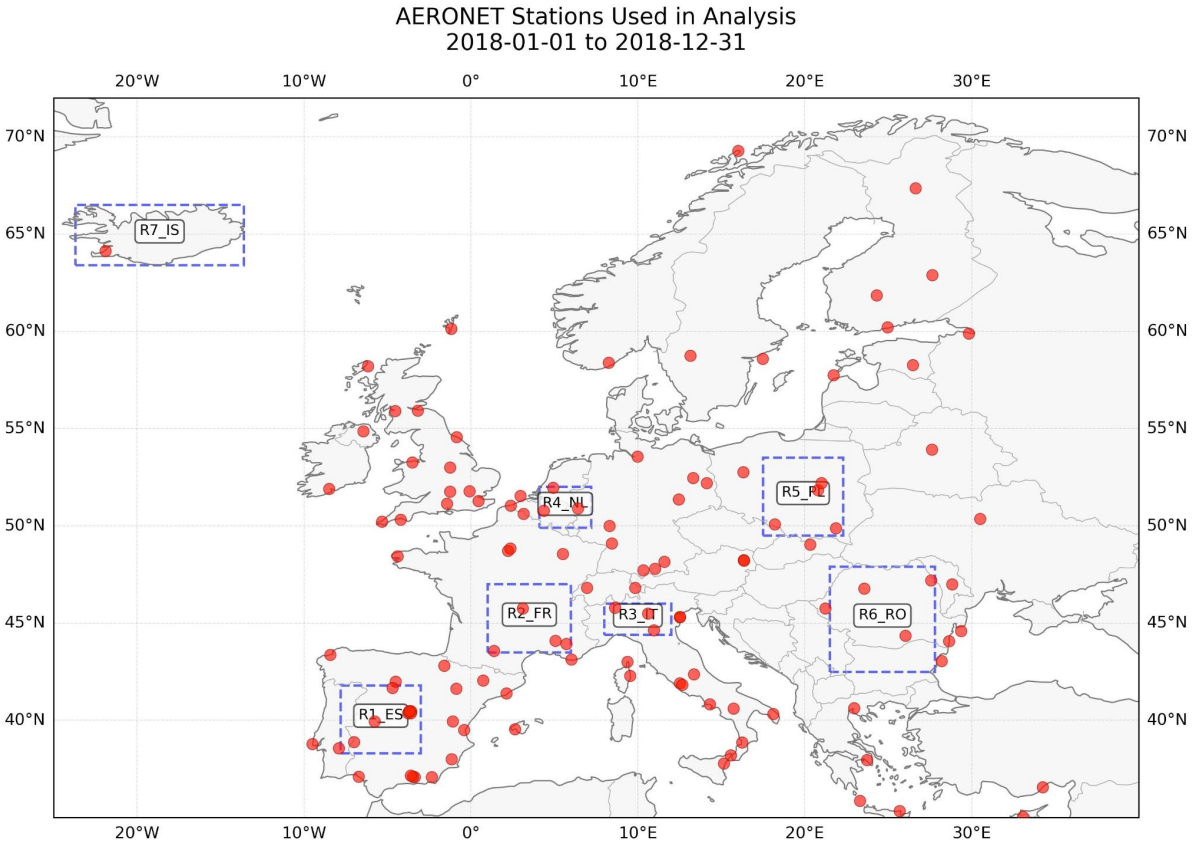

Figure 4 Location and spatial extent of analysed regions for evaluation over Europe and location of AERONET stations used in the analyses

3.1 AERONET network

AERONET data from 117 stations were used for the evaluation of AOD performance for all models. It should be noted that for MINII only AOD@550 was available so in this context the comparison is biased and rather qualitative. On average, all models reproduce well the AOD levels, especially in the second and fourth quarters of 2018. In the first quarter, MINNI was close to AOD, while two other models were similar but lower than observed values. In the third quarter, all models underestimated observed values. The GEM-AQ model showed the lowest values and the largest underestimation among other models; however, peaks in April and May were reproduced correctly. MINNI tends to overestimate in March and December. IFS Compo reproduced best isolated the picks in April, June and October.

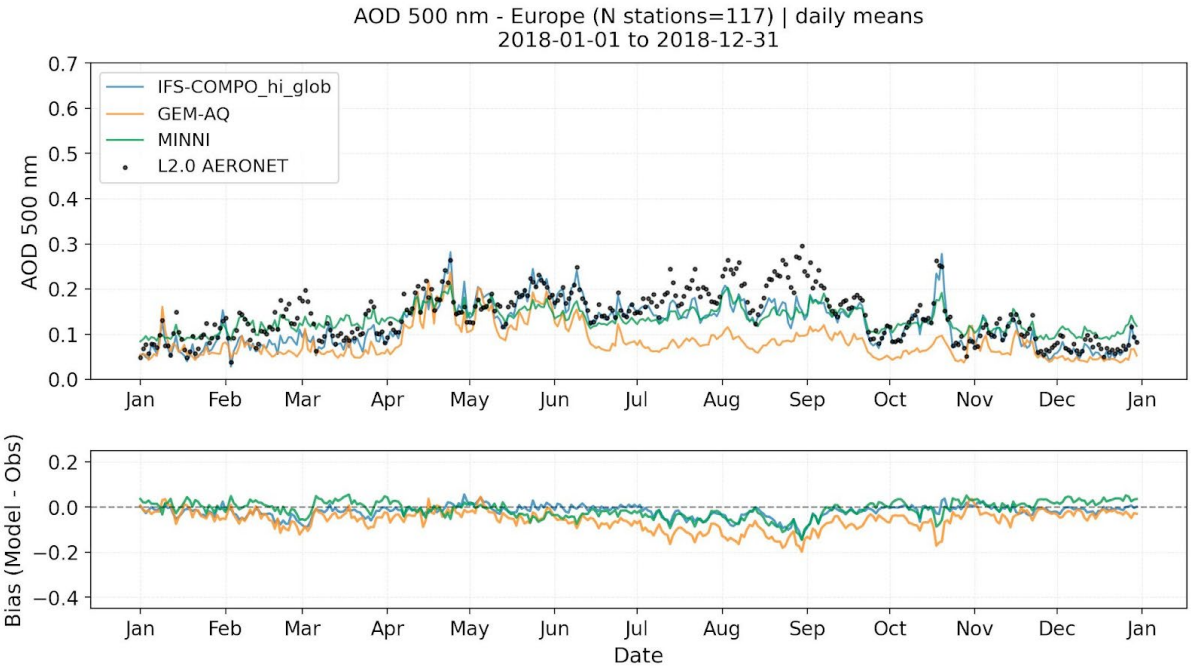

Figure 5 AOD@500 averaged over 117 AERONET stations location

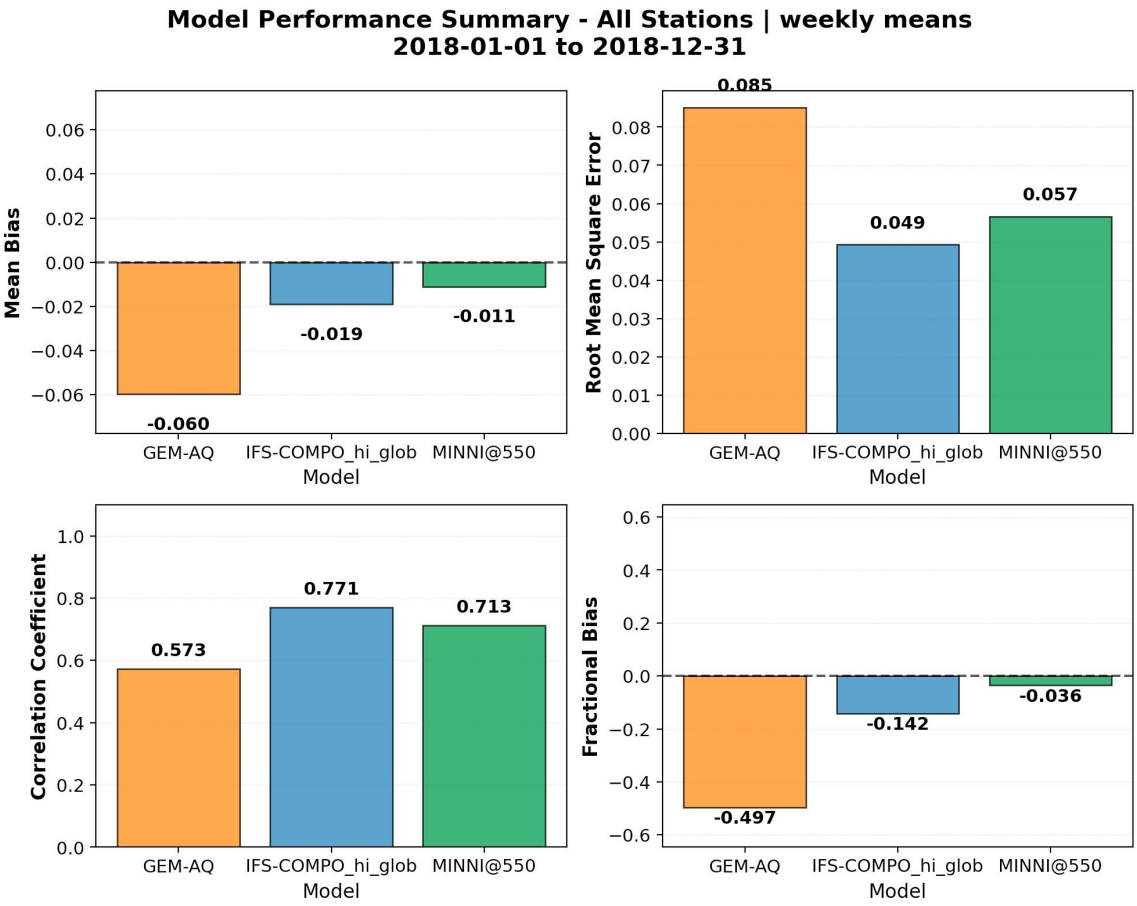

Figure 6 Error statistics calculated for each model based on weekly AOD means (filtering applied)

The regional analysis revealed distinct differences. Over Spain, all models show good agreement. MINNI tends to overestimate AOD from January to April and from October to December. Peaks at the end of April and in mid-November are well reproduced, while summer peaks are underestimated by all models.

Overall, the agreement in France is good. MINNI tends to overestimate during the winter months. GEM-AQ overestimates the peak associated with the end-of-April/beginning-of-May episode. In August, all models underestimate the observed values.

Over Italy, AOD is generally underestimated by all models. IFS-Compo is closest to the observations, particularly in terms of peak representation, especially in October.

A similar pattern is found over the Netherlands and Poland, where relatively high peaks in April, June, and August/September, and in March, April, and August/September, respectively, are not captured. This applies not only to AOD magnitude but also to short-term variability, indicating missing processes.

In south-eastern Europe (Romania), despite an overall underestimation, the agreement between modelled and observed AOD is better.

Over Iceland, only a short period is available. MINNI overestimates AOD values, and none of the models capture the increase at the end of August/beginning of September.

Spain	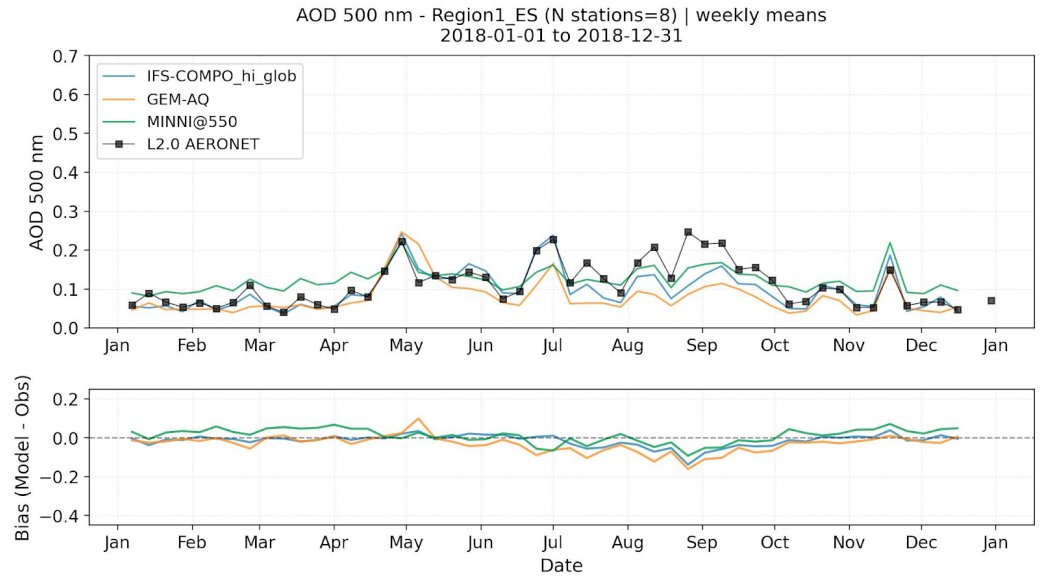

France	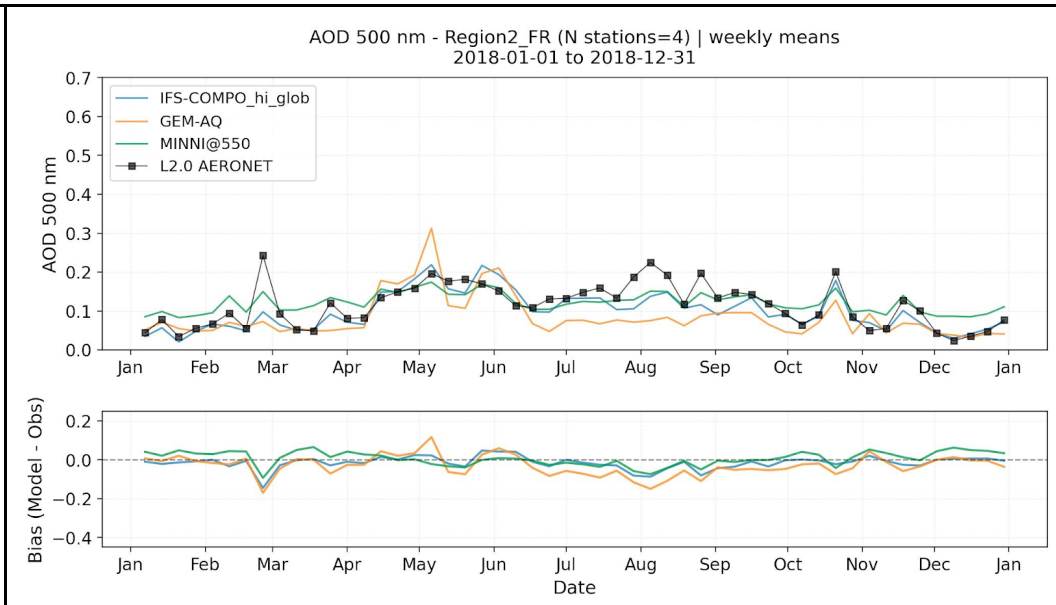
Italy	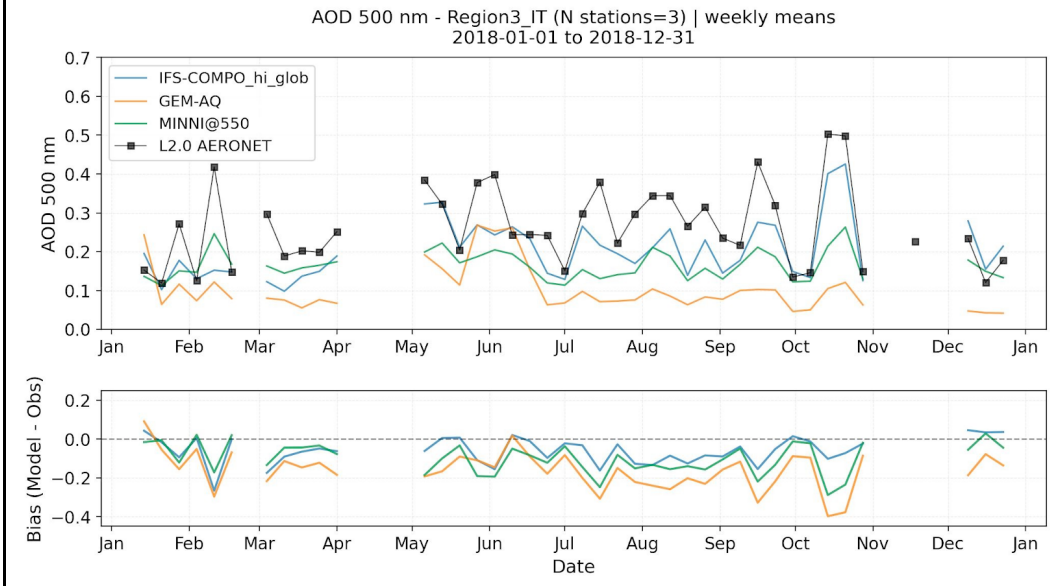
NL	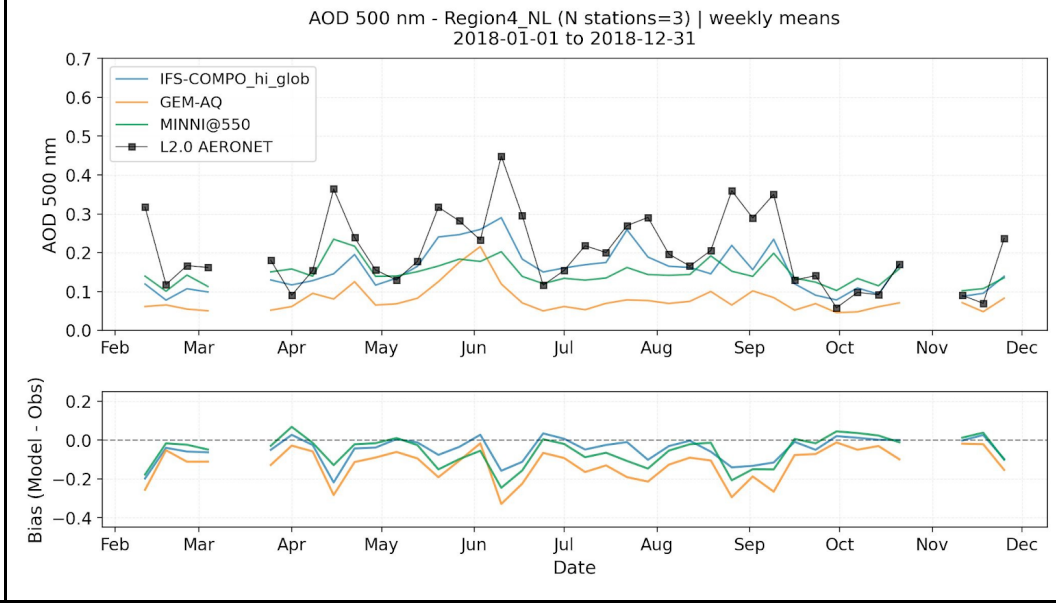

Poland	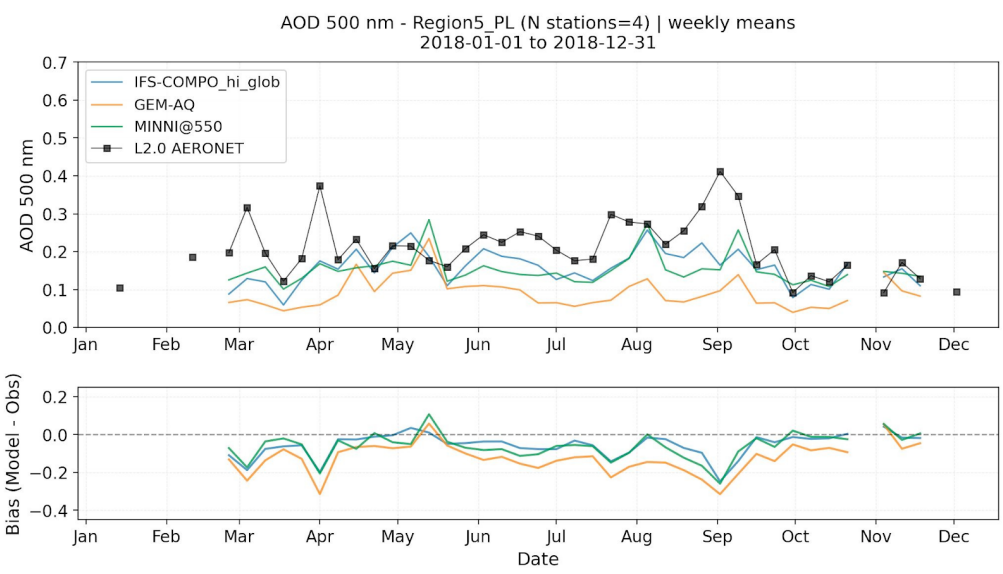
Romania	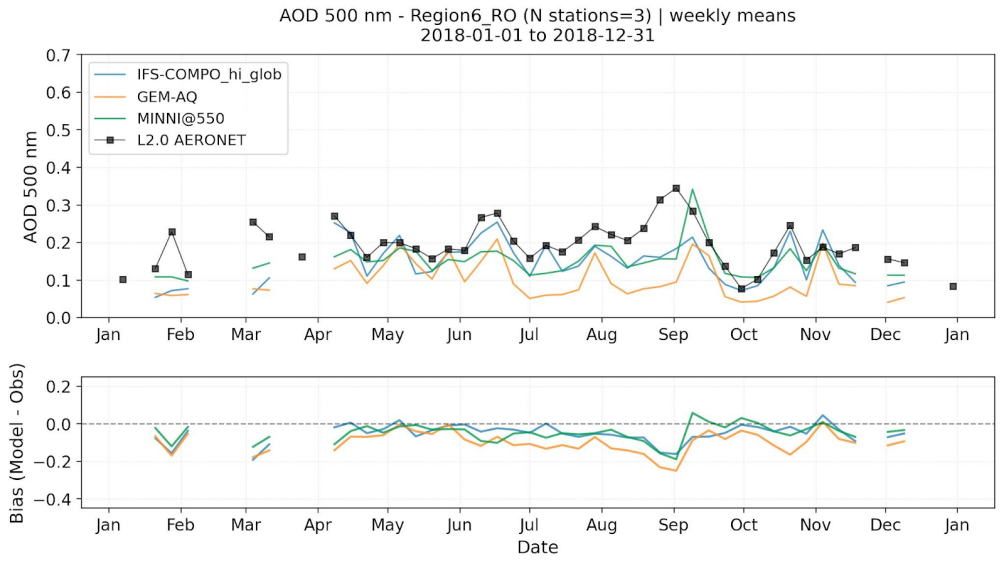
Iceland	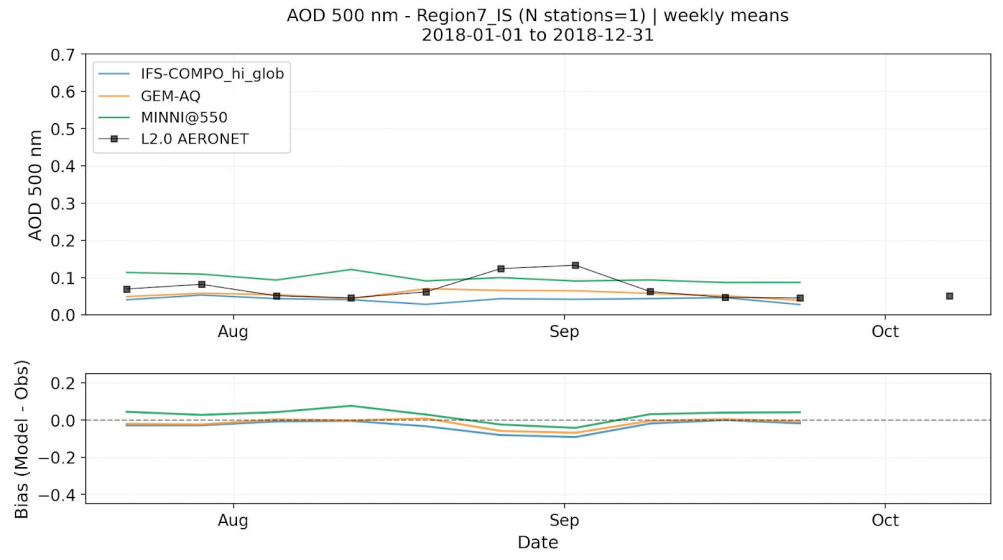

Figure 7 Time series of weakly mean AOD@500 averaged from time series at AERONET stations' location in regions, filtered based on daily observation availability

3.2 MODIS retrieval

The comparison of MODIS observations with modelled aerosol optical depth (AOD) at 550 nm reveals pronounced seasonal variability and systematic differences among the modelling systems. The analysis is based on daily MODIS observations, with filtering applied according to data availability and quality flags.

In January, MODIS-retrieved AOD values over Central and Western Europe are typically in the range of 0.10–0.15. The MINNI model reproduced a similar large-scale spatial distribution, while IFS-COMPO and GEMAQ systematically lower AOD values. Despite this underestimation, both models capture spatial patterns that are comparable.

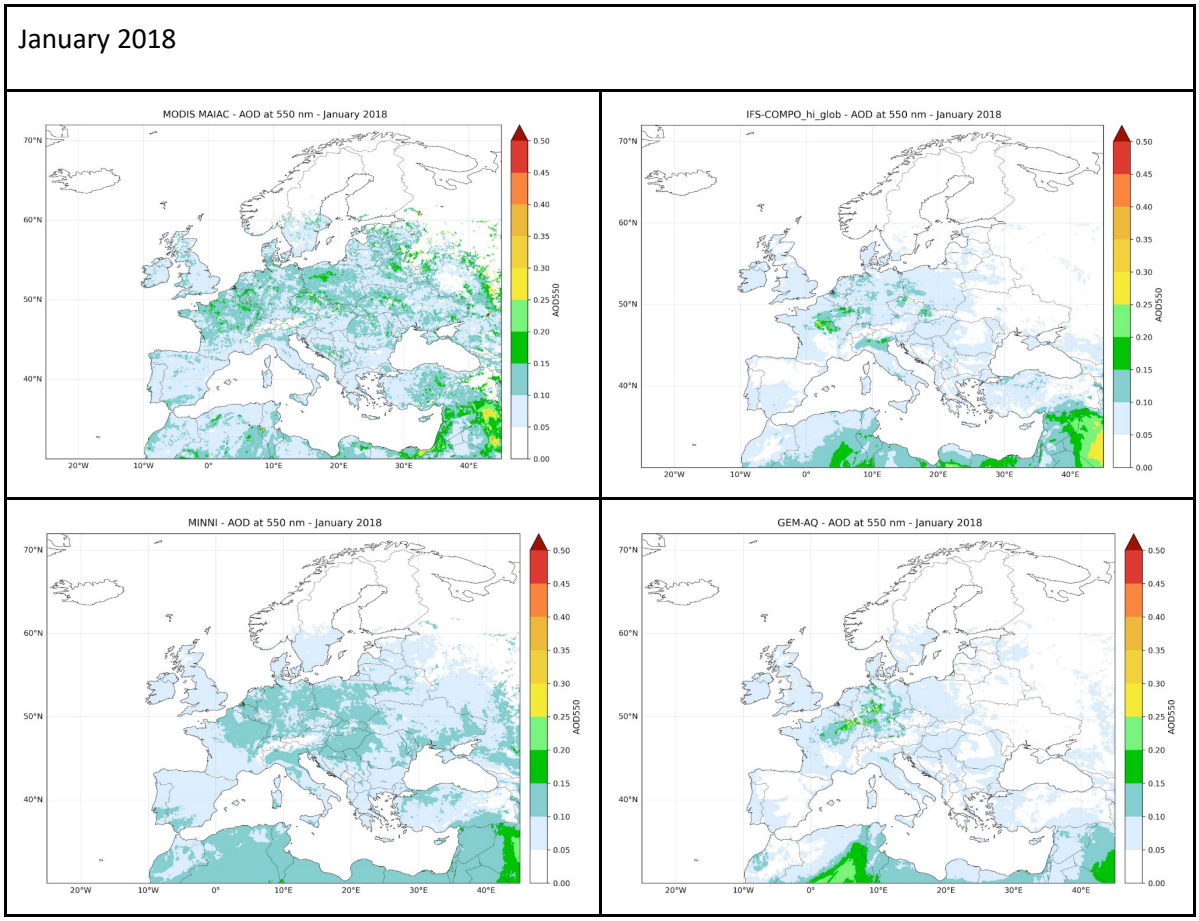

Figure 8.01 AOD@550 January monthly averages calculated for MODIS, IFS-COMPO, MINNI and the GEM-AQ

In February 2018, observed AOD values are higher than in January. Elevated values, reaching approximately 0.20 and locally exceeding this level, are found over Central and Southeastern Europe as well as over the Po Valley. MODIS observations are not available over northern and Eastern Europe during this month. MINNI correctly reproduced the Po Valley hotspot and enhanced AOD over Balkan region. In contrast, IFS-COMPO and the GEM-AQ are characterized by lower AOD values, generally not exceeding 0.10 over most of the domain. Over North Africa, both IFS-COMPO and GEM-AQ simulate a similar spatial pattern.

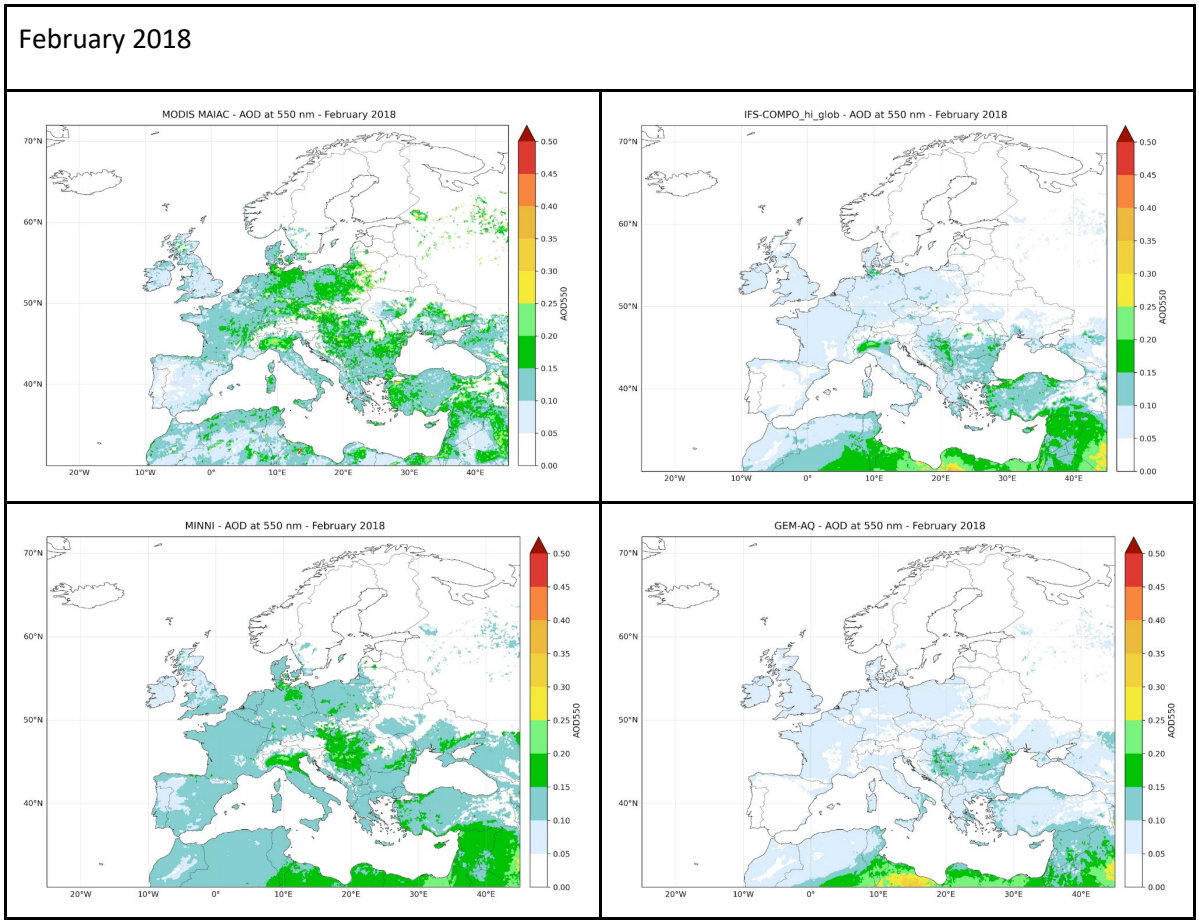

Figure 8.02 AOD@550 February monthly averages calculated for MODIS, IFS-COMPO, MINNI and the GEM-AQ

In March, observed AOD exceeds 0.20 over large parts of Central Europe. MINNi and IFS Compo models reproduced both the spatial pattern and the magnitude of the observed AOD reasonably well. IFS-COMPO represents the spatial pattern over Central Europe and the Po Valley relatively well, but underestimates AOD over Western Europe. GEM-AQ shows a pronounced underestimation, with its highest values located over North Africa.

March 2018

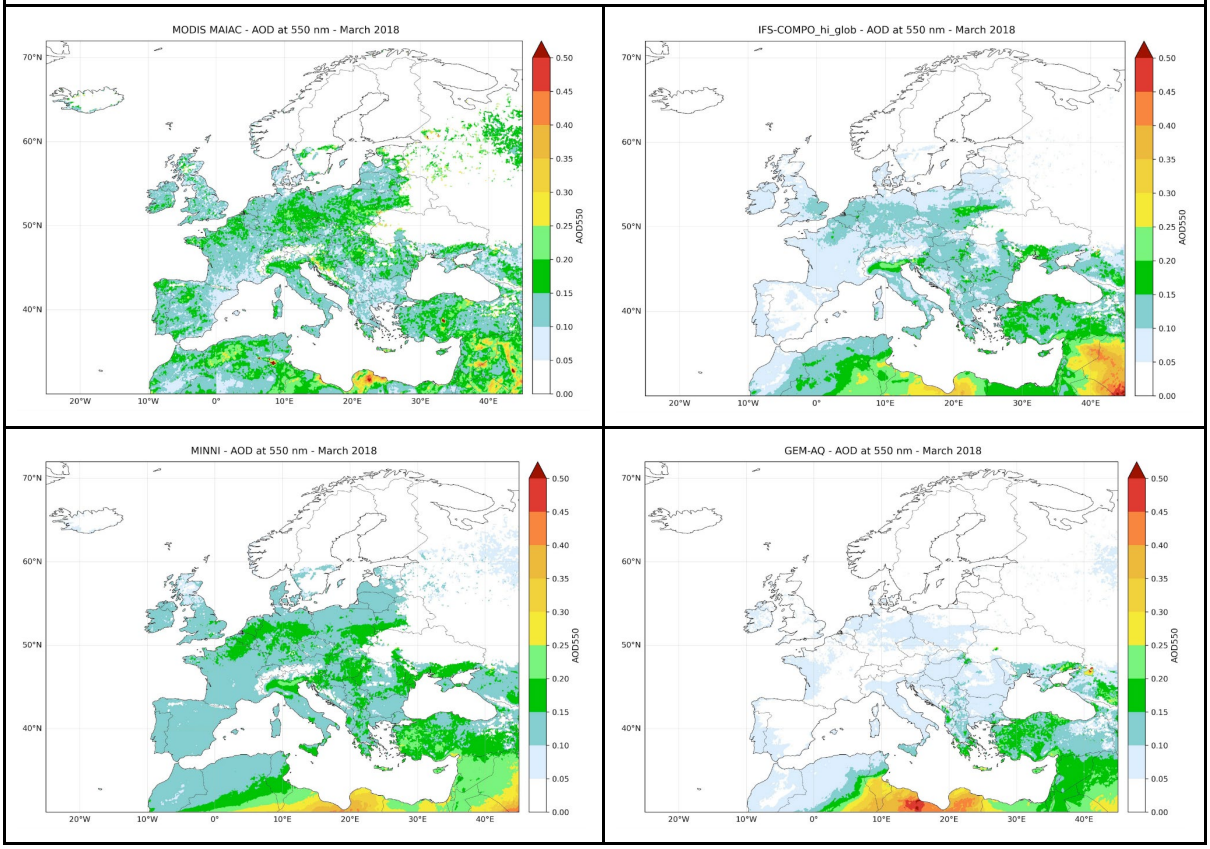

Figure 8.03 AOD@550 March monthly averages calculated for MODIS, IFS-COMPO, MINNI and the GEM-AQ

In April, observed AOD values increased over the central and northern parts of the domain as well as over the Iberian Peninsula. Elevated AOD over the Iberian Peninsula and the Netherlands is reproduced well by all models. Over Central Europe, GEM-AQ continues to underestimate AOD. IFS-COMPO exhibits slightly higher spatial variability. However, the elevated AOD simulated over the southern part of the domain by MINNI and IFS Compo, particularly over the Balkan countries and Greece, is not supported by observations, which indicate lower values in this region. It should be noted that MODIS observations do not confirm very high AOD values appearing near the southern edges of the domain, which may be related to satellite data post-processing effects.

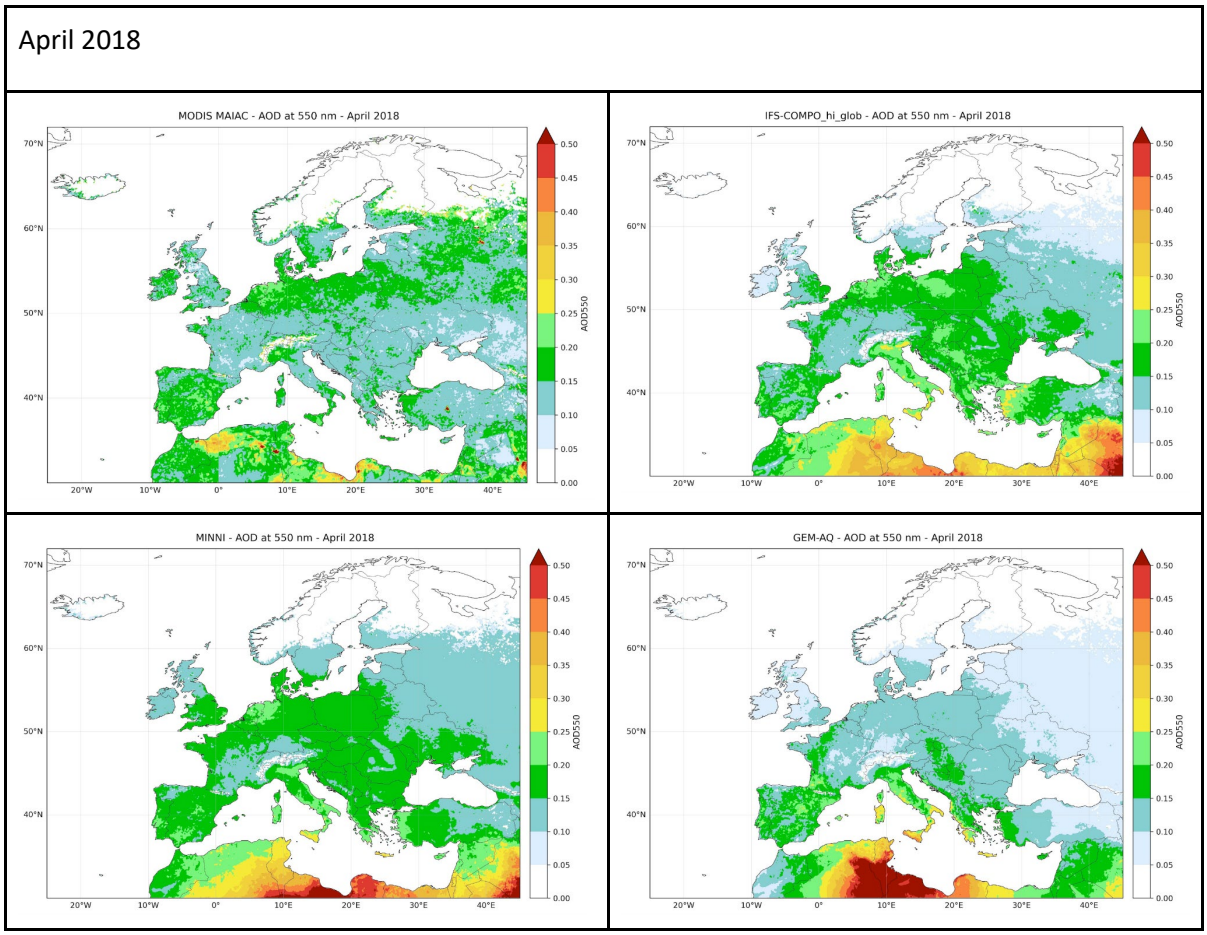

Figure 8.04 AOD@550 April monthly averages calculated for MODIS, IFS-COMPO, MINNI and the GEM-AQ

In May, MODIS observations are available over the entire domain. The lowest AOD values are observed over Scandinavia and the northern part of the domain, while higher values occur over Central and Southern Europe. For this month, the MINNI model shows generally agreement, while an overestimation is evident in the eastern part of the domain. A similar overestimation in Eastern Europe is found for GEMAQ, whereas IFS-COMPO exhibits a weaker signal in this region. Overall, in May, all models were quite close to the observations.

May 2018

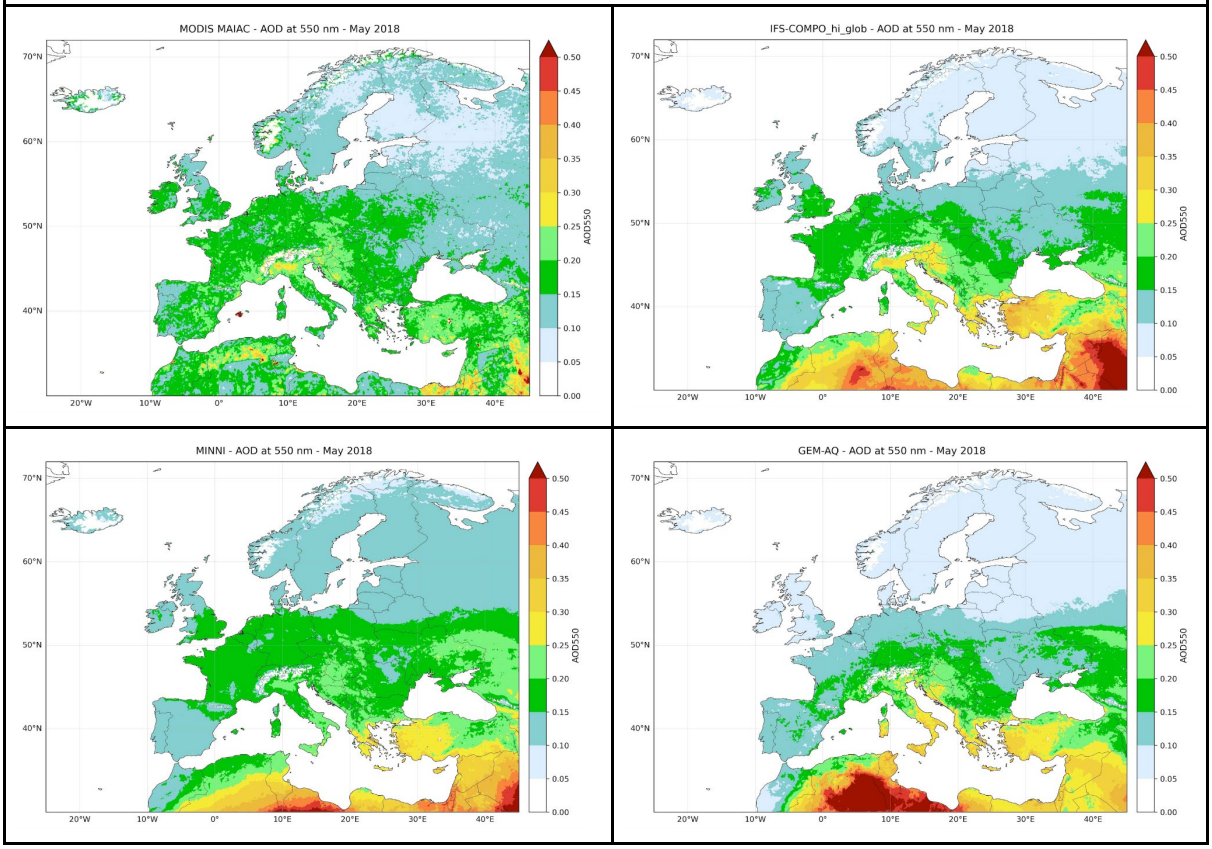

Figure 8.05 AOD@550 May monthly averages calculated for MODIS, IFS-COMPO, MINNI and the GEM-AQ

In June, the highest observed AOD values are located in the central part of the domain, extending over Central and Southeastern Europe. All models reproduce the presence of enhanced AOD in this region; however, none correctly capture the precise location of the maximum values. In IFS-COMPO and GEM-AQ, the highest AOD is shifted towards the Balkan countries. The MINNI model does not reproduce a single, well-defined region of enhanced AOD, and values over Poland and Germany are generally underestimated.

June 2018

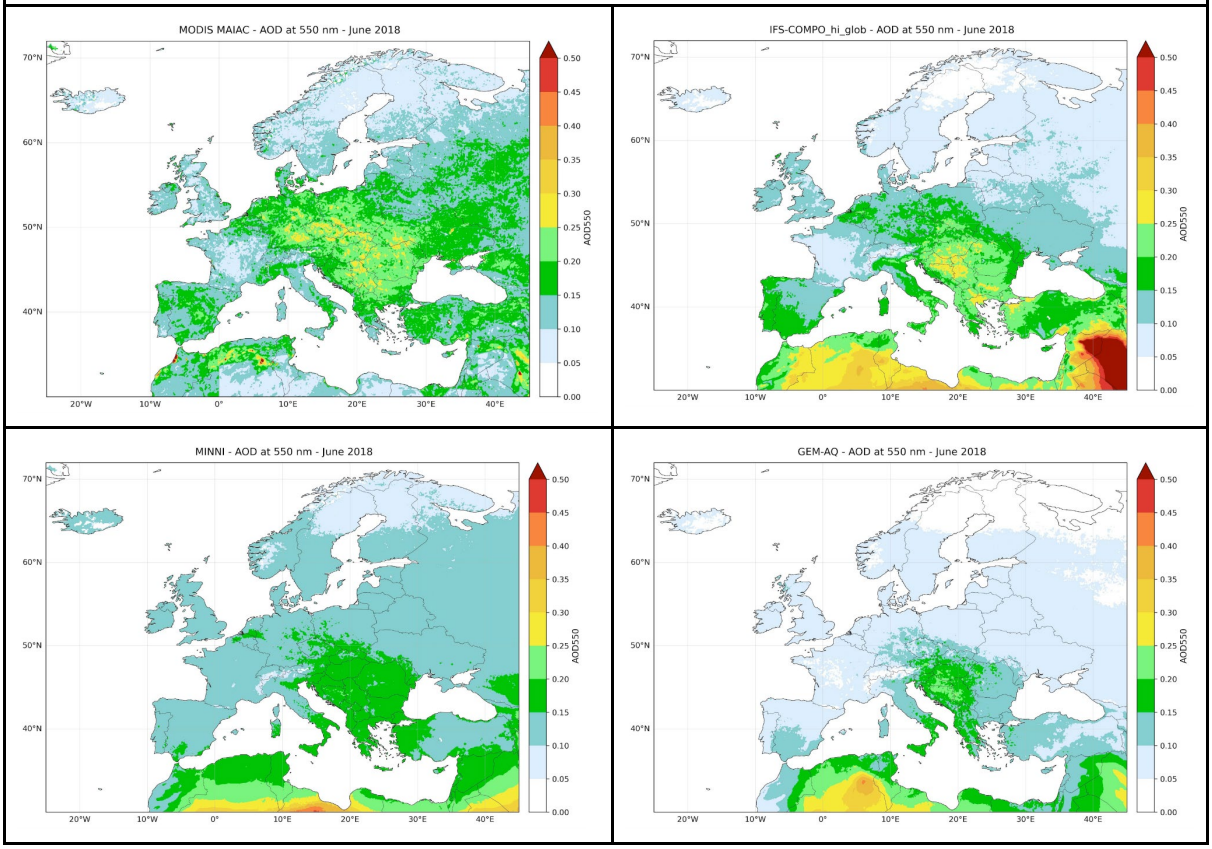

Figure 8.06 AOD@550 June monthly averages calculated for MODIS, IFS-COMPO, MINNI and the GEM-AQ

In July, MODIS observations show elevated AOD values over Eastern Europe, with the highest values predominantly over Ukraine. This pattern is partly reproduced by all modelling systems. The ensemble mean indicates a strong inflow from the eastern direction, likely originating from over the deserts near the Caspian Sea region, although this signal appears to be overestimated. In IFS-COMPO, enhanced AOD values are also present along the eastern edge of the domain, but with a weaker magnitude than in the case of MINNI models. A similar, weaker signature of eastern inflow is simulated by GEM-AQ. At the same time, all models underestimate AOD over most of Europe. In the ensemble mean, AOD over western and northern Europe is spatially uniform and lacks distinct patterns. In GEM-AQ, AOD values are consistently underestimated and generally do not exceed 0.10. IFS-COMPO correctly reproduces enhanced AOD over the Netherlands. Over North Africa, AOD is overestimated by IFS-COMPO and the MINNI model, while GEM-AQ shows better agreement with observations.

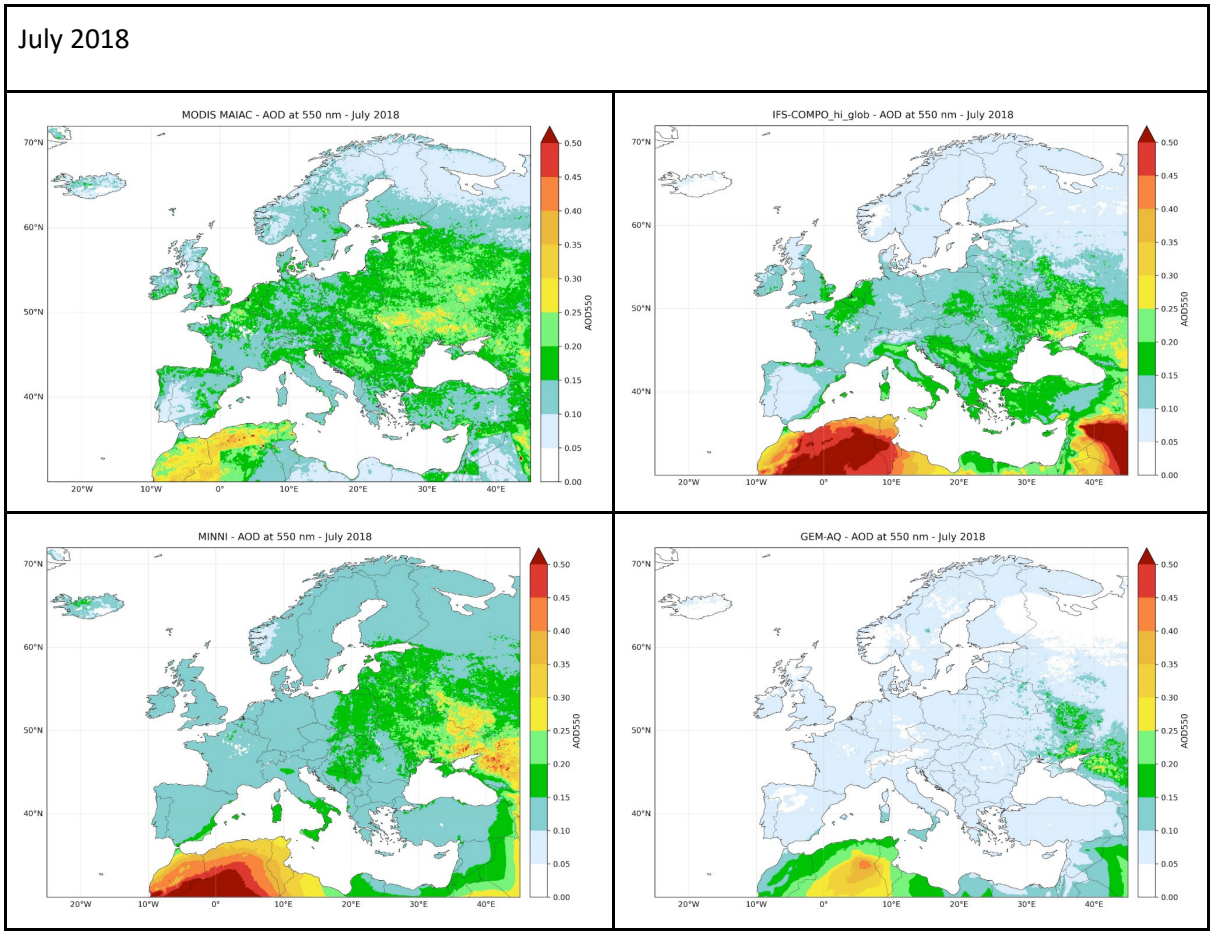

Figure 8.07 AOD@550 July monthly averages calculated for MODIS, IFS-COMPO, MINNI and the GEM-AQ

In August, large discrepancies are observed between MODIS retrievals and modelled AOD fields. Observations indicate several regions with AOD values exceeding 0.20 over Central Europe, as well as over Spain, Greece, and Turkey. These features are not reproduced by the models. In MINNI, AOD values are typically in the range of 0.10–0.15, with regions over Spain and Central Europe reaching approximately 0.20. In GEM-AQ, AOD values do not exceed 0.10 over most of the domain, with slightly higher values (up to about 0.15) only over Spain. In contrast, IFS-COMPO simulates higher AOD over Central Europe, including localized hotspots exceeding 0.25 that are not supported by observations, as well as elevated values over the Balkan region. In IFS-COMPO, AOD values over northern Europe are underestimated.

August 2018

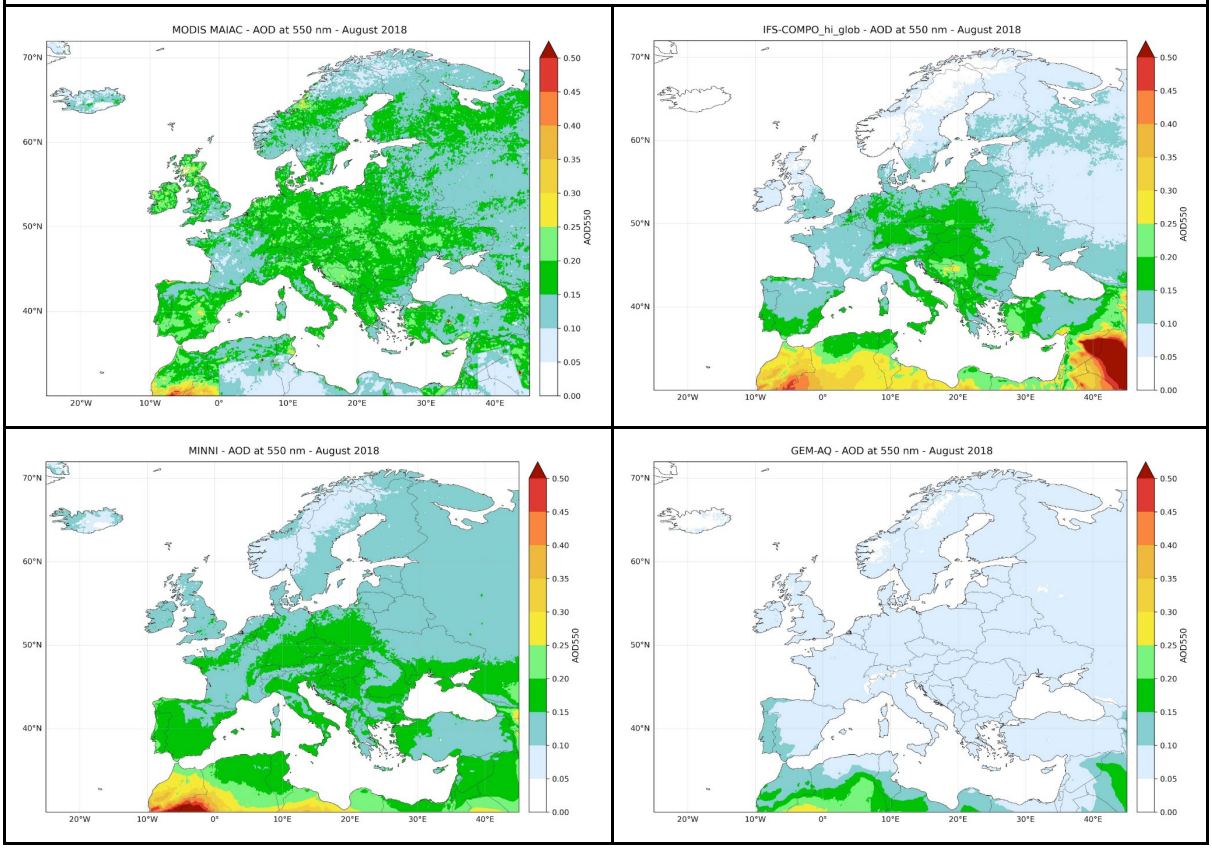

Figure 8.08 AOD@550 August monthly averages calculated for MODIS, IFS-COMPO, MINNI and the GEM-AQ

In September, the observed AOD distribution is reproduced relatively well by IFS-COMPO, both in terms of spatial pattern and magnitude. Lower AOD values are found over western Europe, while moderately elevated values occur over Central and Eastern Europe, generally not exceeding 0.20. GEM-AQ underestimates the observed pattern across much of the domain. In MINNI, inflow from the east is substantially overestimated.

September 2018

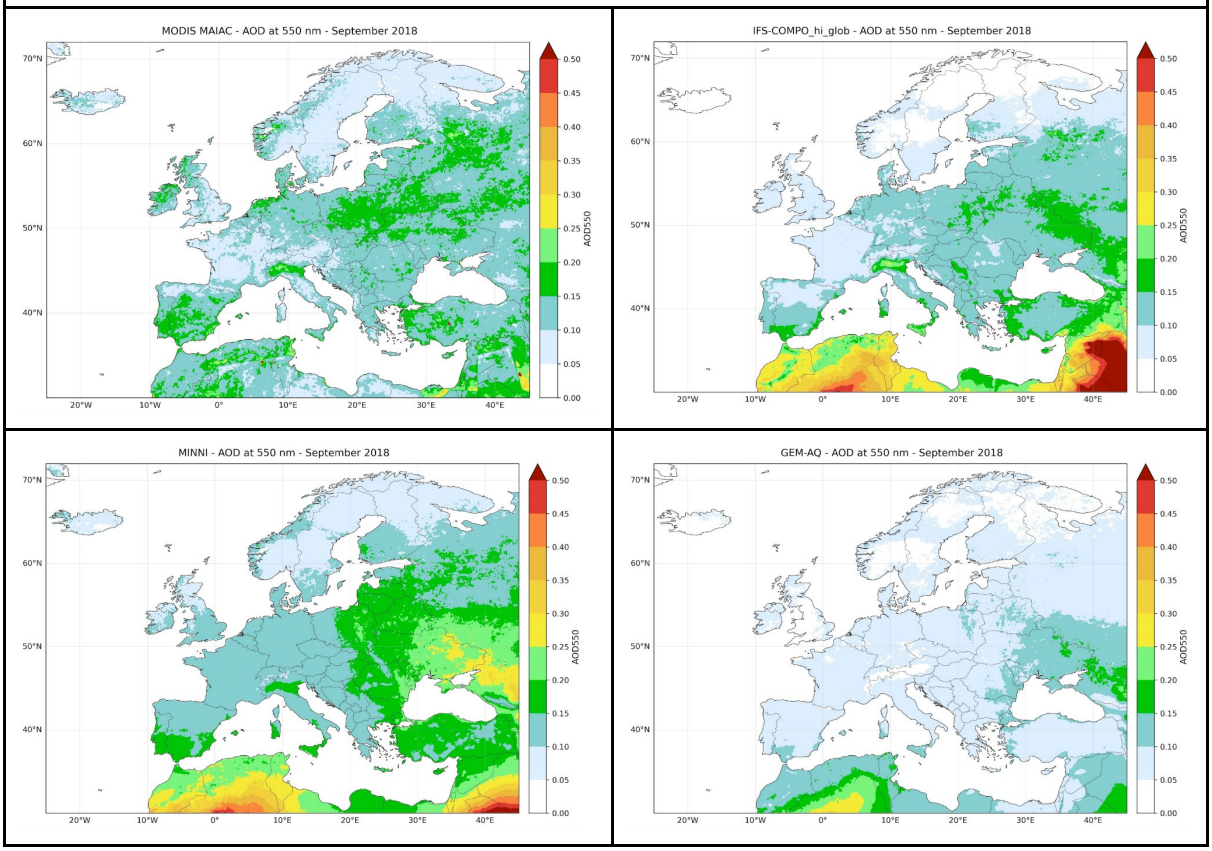

Figure 8.09 AOD@550 September monthly averages calculated for MODIS, IFS-COMPO, MINNI and the GEM-AQ

In October, the observed AOD values are mostly below 0.10, with some regions reaching up to 0.15. This range is reproduced reasonably well by IFS-COMPO; however, AOD over Central Europe and the Balkan region is overestimated. GEM-AQ captures AOD magnitude relatively well, though with regional underestimation in Central Europe and overestimation in Eastern Europe. In MINNI, overestimation is pronounced, with simulated AOD values exceeding 0.20 in several regions, which is not supported by observations.

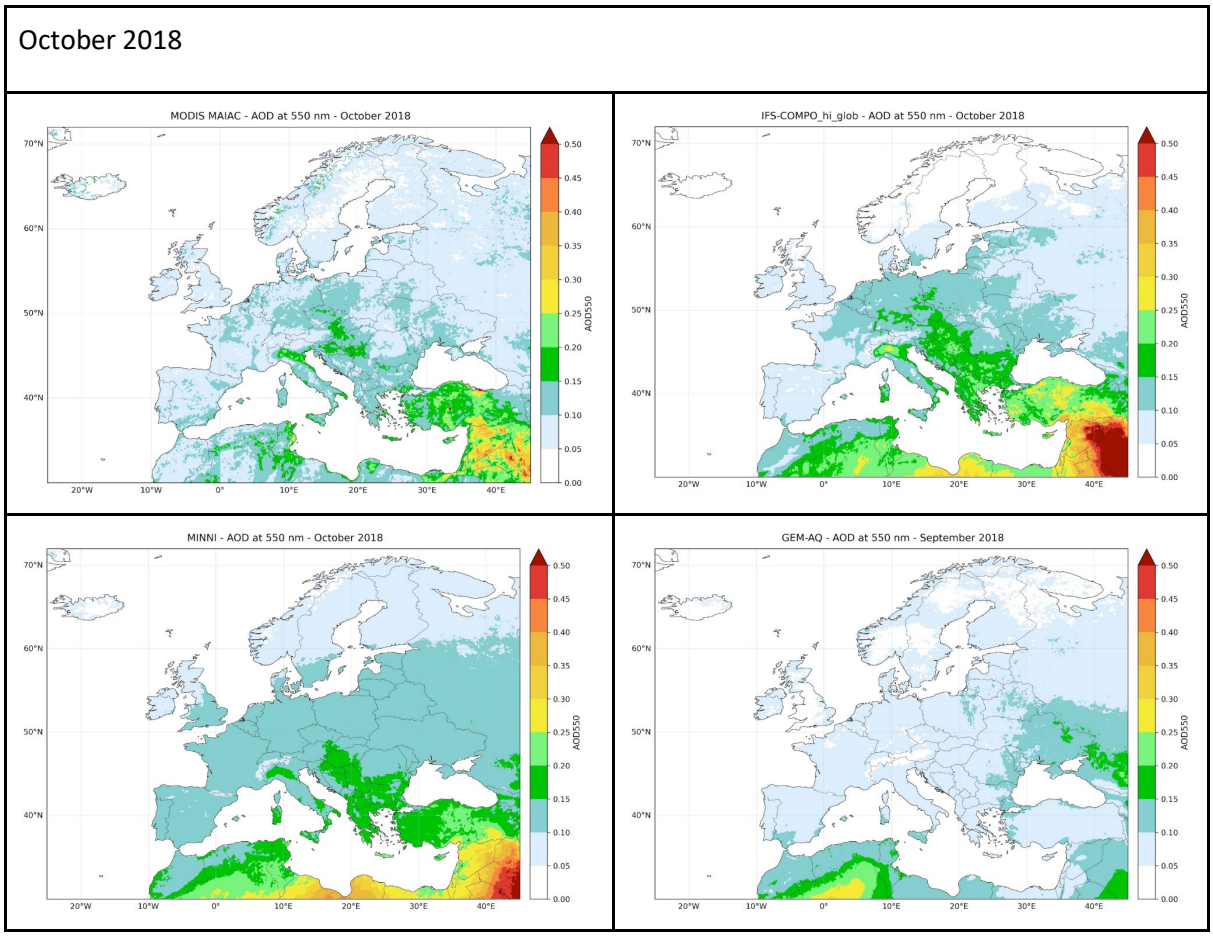

Figure 8.10 AOD@550 October monthly averages calculated for MODIS, IFS-COMPO, MINNI and the GEM-AQ

In November, the agreement between IFS-COMPO and MODIS observations is very good, both in terms of spatial distribution and variability range. Most regional features are well reproduced, although AOD over Spain is underestimated. MINNI generally overestimates AOD across the domain, while GEM-AQ tends to underestimate values.

November 2018

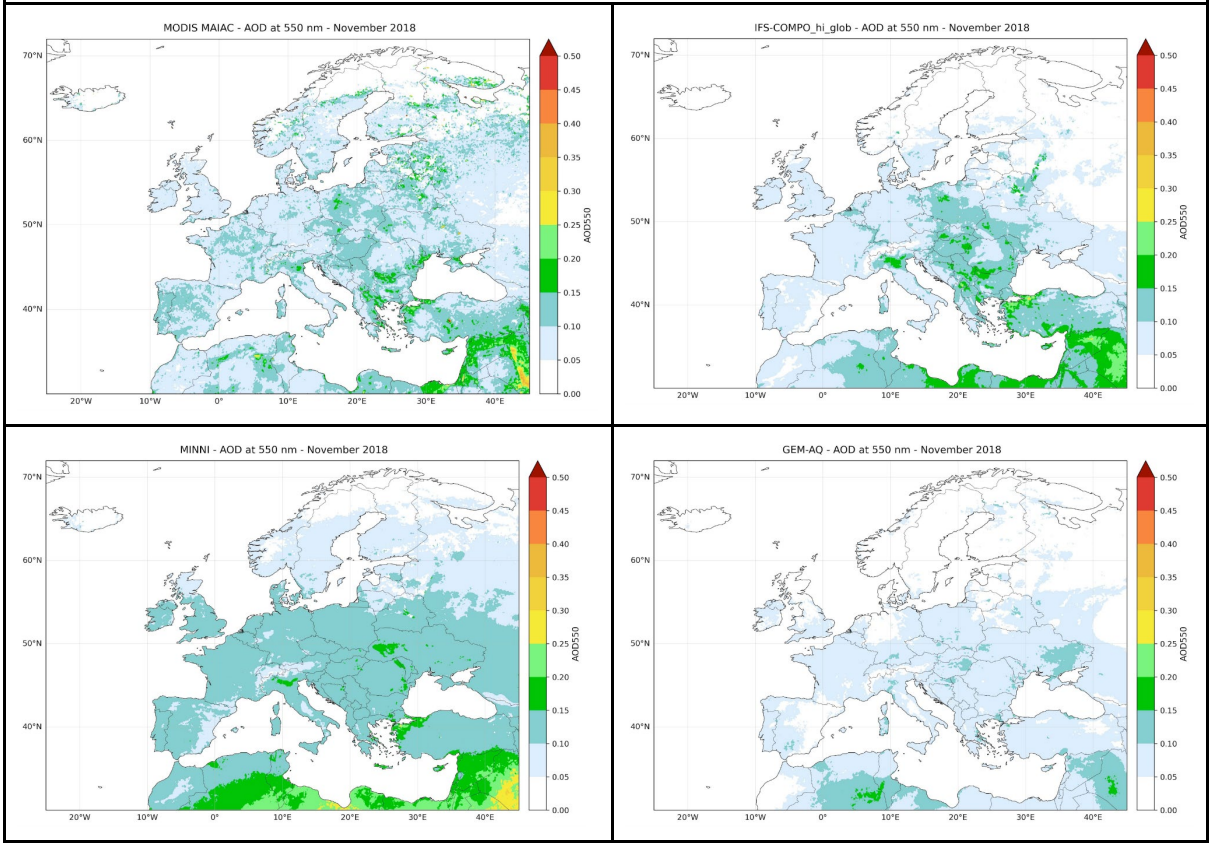

Figure 8.11 AOD@550 November monthly averages calculated for MODIS, IFS-COMPO, MINNI and the GEM-AQ

In December, both GEM-AQ and IFS-COMPO underestimate observed AOD over much of Europe. In IFS-COMPO, a localized hotspot is present, but its magnitude is weaker than suggested by observations. For this month, MINNI shows closer agreement with MODIS than the other models; however, it overestimates AOD over western Europe, particularly over Spain and North Africa.

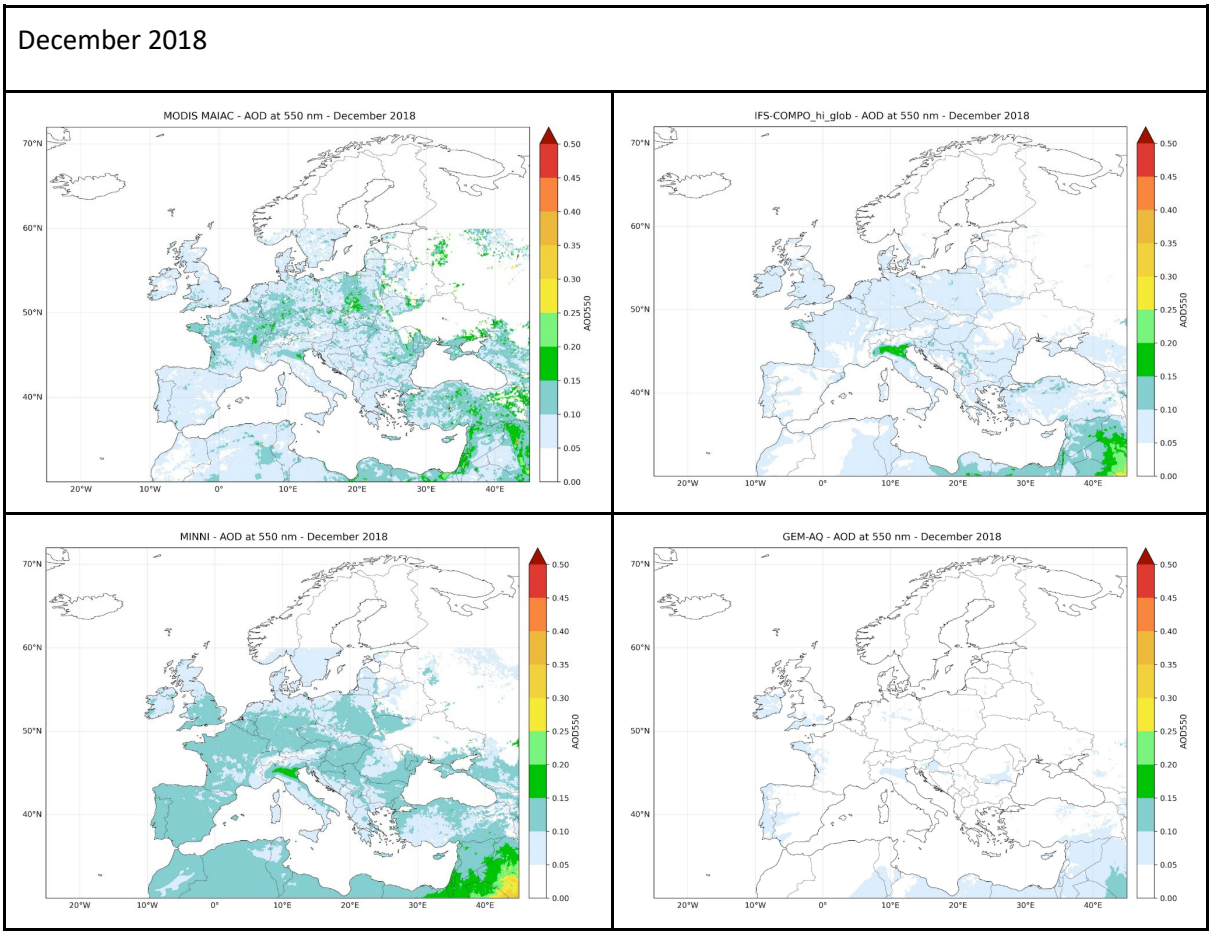

Figure 8.12 AOD@550 December monthly averages calculated for MODIS, IFS-COMPO, MINNI and the GEM-AQ

The comparison of MODIS observations with modelled AOD at 550 nm reveals several systematic features that are consistent across the three modelling systems considered in this study (IFS-COMPO, GEMAQ, and MINNI).

All three models show a tendency to overestimate AOD values during the autumn months, particularly in October and November. During this period, observed AOD values are mostly below 0.10, whereas the models frequently simulate values exceeding 0.15 and locally reaching or exceeding 0.20, indicating a positive bias under late-year conditions.

The three models also tend to overestimate aerosol inflow from the eastern boundary of the domain. This feature appears persistently in the simulations but is supported by observations only in July, when elevated AOD values are detected over Eastern Europe, particularly over Ukraine. Outside this month, the simulated eastern inflow is not confirmed by MODIS observations, suggesting an overestimation of boundary contributions in the models.

All three models do not to reproduce elevated AOD values in the eastern part of the domain during several months when observations are available. In particular, enhanced AOD is observed in April,

June, July, and August, including elevated values extending into Scandinavia during summer, but these features are largely absent or strongly underestimated in the simulations. This indicates a systematic underrepresentation of aerosol load in eastern and northeastern Europe during the warm season.

Over North Africa, the simulated AOD signal is generally stronger than the MODIS observations in all three models. It remains unclear whether this discrepancy is related to an overestimation of dust source strength in the models or to limitations and post-processing of MODIS retrievals, as discussed in the section describing the MODIS data. This uncertainty should be taken into account when interpreting the North African signal.

Elevated AOD values over Central Europe, the Benelux countries, and the Po Valley indicate a strong contribution from anthropogenic emissions, which is particularly evident in the Po Valley. However, in most months, the Po Valley signal is overestimated by all three models, suggesting that anthropogenic source strengths, aerosol formation, or removal processes may not be fully balanced in the simulations.

A distinct hotspot over the Netherlands is observed in April and again in July, highlighting the role of regional emissions and favourable meteorological conditions. In contrast, during winter months, the observed AOD signal is generally weaker and more localized, while the modelled fields tend to be smoother and, in some cases, biased high.

Based on monthly mean AOD over Europe, the overall variability is reasonably well reproduced by the models, although systematic differences among them are evident.

For the MINNI model, during the first quarter of 2018, monthly averages across Europe are closest to the observations. The GEM-AQ model slightly underestimates AOD in April and May but remains the closest to observations for these months. The IFS-COMPO model reproduces the European mean AOD most accurately in June, July, September, and November.

A negative bias is present in all models during several months. Notably, during August and the last quarter of the year (September–December), the models tend to overestimate AOD relative to observations; a similar overestimation occurs in April and May.

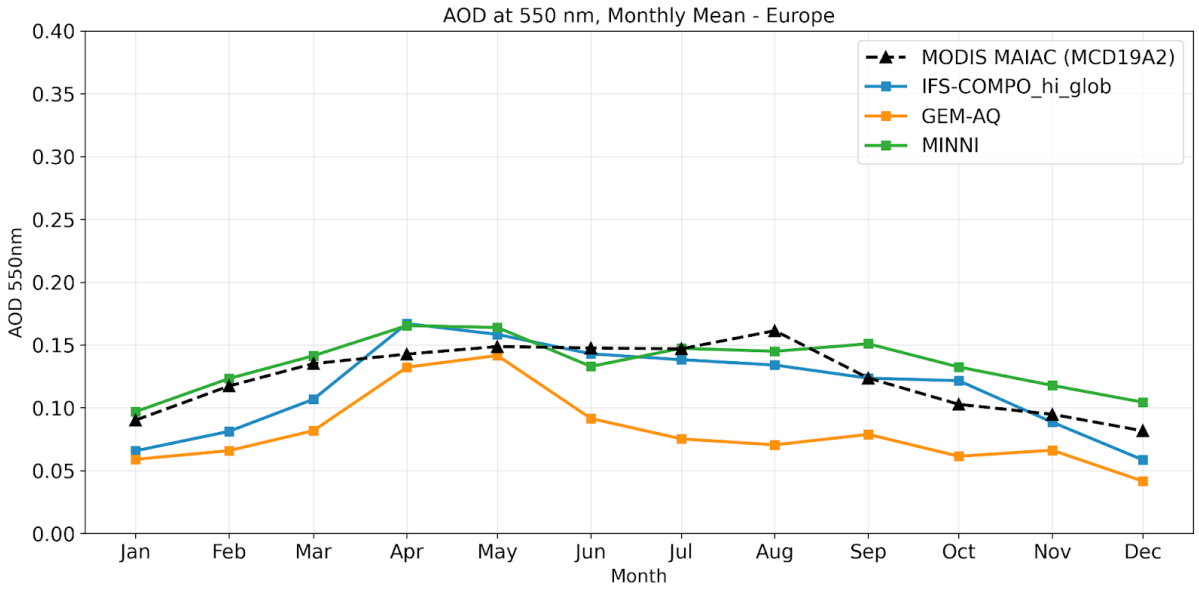

Figure 9 AOD@550 monthly averages calculated for MODIS, IFS-COMPO, MINNI and the GEM-AQ

At the regional level, MINNI generally shows slight overestimation, whereas GEM-AQ exhibits slight underestimation. IFS-COMPO underestimates AOD in most regions except Italy. For GEM-AQ, underestimation is particularly strong for Iceland throughout the year, while other regions display diverse patterns. Positive bias in GEM-AQ is limited, appearing only in Italy in April and Romania in May. MINNI shows systematic overestimation, especially from September to December. GEM-AQ exhibits the strongest negative biases in June, July, and August across most regions, with additional underestimation in Italy in February and across most regions in March.

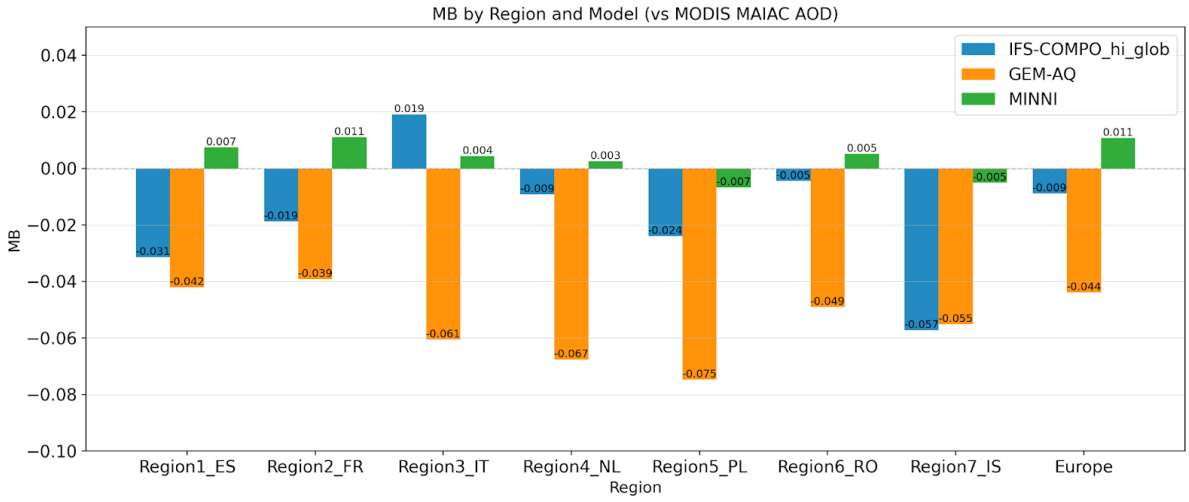

Figure 10 AOD@550 annual biases calculated for IFS-COMPO, MINNI and the GEM-AQ against MODIS for each region

Overall, the time series comparison highlights model-dependent seasonal biases. IFS-COMPO performs best in selected months, MINNI tends to overestimate later in the year, and GEM-AQ generally shows underestimation across most regions. These patterns are consistent with the regional and monthly variability observed in the AOD datasets.

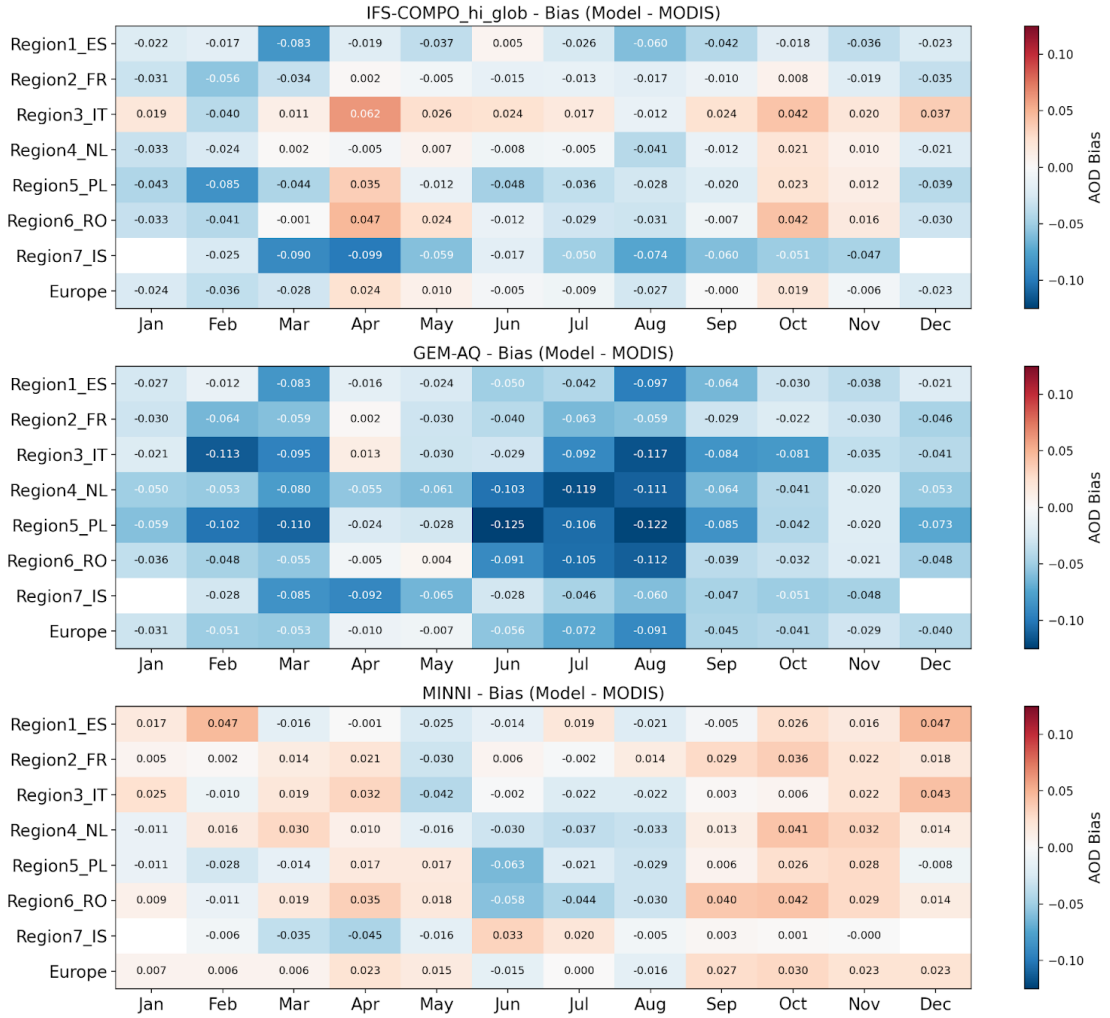

Figure 11 AOD@550 monthly biases calculated for IFS-COMPO, MINNI and the GEM-AQ against MODIS for each region and each month of 2018

The correlation between MODIS AOD observations and model results varies considerably depending on both region and model characteristics. For all models, the lowest correlation is found over Iceland, reflecting difficulties in reproducing AOD variability in this region. Among the models, GEM-AQ shows the highest correlation over Iceland, reaching values of approximately 0.3, although this remains low in absolute terms.

Overall, the highest correlations for most regions are obtained with IFS-COMPO, indicating its better capability to reproduce observed temporal variability at the regional scale in spite of the global emission dataset used in the simulation. For Spain and Italy, the MINNI model shows slightly higher correlation than the other models, highlighting the importance of regionally representative emission inventories used in this system.

For the GEM-AQ while relatively high correlations are obtained over Spain and France, slightly lower values are found over Italy and the Netherlands. The weakest performance of GEM-AQ is observed over Poland, suggesting a systematic underestimation of AOD or the absence of relevant processes affecting aerosol variability in this region.

When considering Europe as a whole, the correlation between modelled and observed AOD ranges from approximately 0.65 for GEM-AQ to 0.83 for IFS-COMPO.

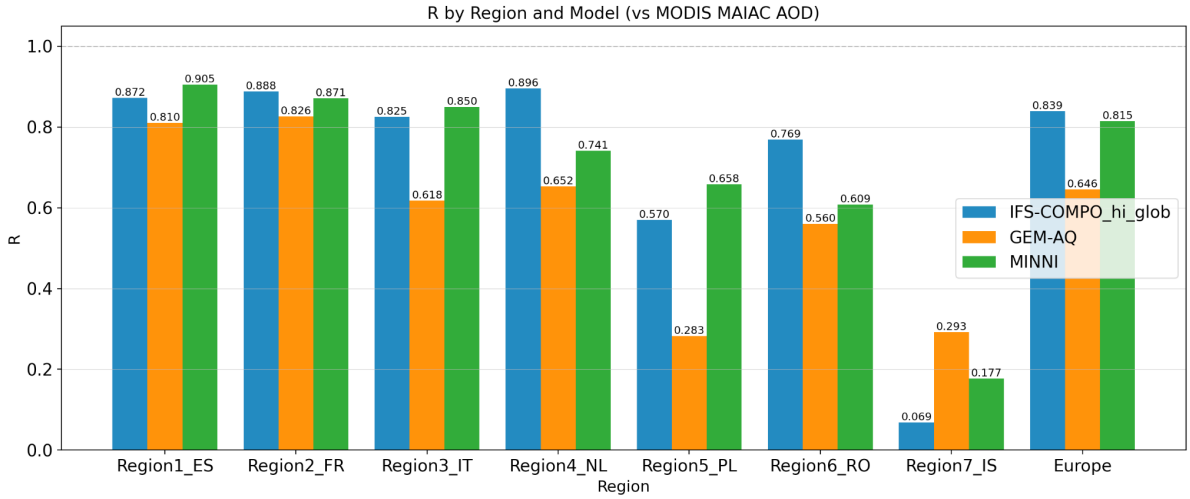

Figure 10 AOD@550 correlation calculated for IFS-COMPO, MINNI and the GEM-AQ against MODIS for each region

4. Conclusion

This report extends the previous analysis of the global and regional models' performance for PM10 and PM2.5 by evaluating aerosol optical depth (AOD) for 2018 using one global model (IFS-COMPO) and two regional models (GEM-AQ and MINNI). The regional simulations were driven by IFS-COMPO meteorology and chemical boundary conditions. AOD calculations rely on a specific model-dependent approach.

The intercomparison of monthly average AOD spatial patterns indicates that all models capture major processes controlling AOD, such as dust intrusions and anthropogenic emissions, but systematic differences exist in magnitude and seasonality. Model-to-model correlations are highest in spring and summer, while winter and transitional periods show larger discrepancies.

Evaluation against AERONET data from 117 stations confirms that all models reproduce the general AOD@500 levels across Europe, with the best performance during the second and fourth quarters of 2018. Regionally, agreement is good over Spain and France, reflecting a correct representation of dust outbreaks, while AOD is systematically underestimated over Italy, the Netherlands, and Poland. Over south-eastern Europe, underestimation is smaller, whereas over Iceland, MINNI overestimates AOD, and all models do not to capture observed peaks. Specific regional features suggest additional sources or processes, such as sea salt over the North Sea and Atlantic, or biomass burning long range transport from over North America, which may not be fully accounted for.

Comparison with MODIS AOD at 550 nm highlights further consistent features across models. All three tend to overestimate autumn AOD, particularly in October–November, and overrepresent aerosol inflow from the eastern boundary, only partially supported by observations. Elevated AOD in eastern and north-eastern Europe during spring and summer is underrepresented, while over North Africa, simulated AOD exceeds observations, reflecting possible model or observational uncertainties. Anthropogenic hotspots over Central Europe, the Benelux, and the Po Valley are generally captured, but AOD is often overestimated, particularly in the Po Valley.

In conclusion, GEM-AQ tends to underestimate, MINNI shows late-year overestimation, and IFS-COMPO best represents short-term peaks. These results emphasize the need for careful interpretation of modelled AOD, accounting for seasonal variability, regional differences, and limitations in the representation of chemical components and aerosol transport. The formulation of the optical module plays a critical role in the representation of aerosol optical depth. The relatively simple parameterization implemented in the MINNI model demonstrates robust performance. In contrast, the more complex optical module in GEM-AQ does not explicitly account for biomass-burning-related aerosol tracers, as these emissions are introduced only as total PMWF, which may contribute to the observed systematic underestimation. Further analysis of PM10 and aerosol component vertical profiles would be required to better understand the sources of the remaining discrepancies.

Document History

Version	Author(s)	Date	Changes
1.0	Rose-Cloé Meyer, Samuel Remy, Joanna Strużewska, Jacek Kaminski, Tomasz Przybyła, Damian Mochocki	28/01/2026	Initial version

Internal Review History

Internal Reviewers	Date	Comments